

IEEE COPYRIGHT NOTICE

This work has been submitted to the IEEE for possible publication. Copyright may be transferred without notice, after which this version may no longer be accessible.

Quality of Control Assessment for Tactile Internet based Cyber-Physical Systems

Kurian Polachan*, Joydeep Pal †, Chandramani Singh‡, and Prabhakar T V§

Indian Institute of Science, Bangalore, India

{*kurian, †joydeppal, ‡chandra, §tvprabs}@iisc.ac.in

Abstract

We evolve a methodology and define a metric to evaluate Tactile Internet based Cyber-Physical Systems or Tactile Cyber-Physical Systems (TCPS). Towards this goal, we adopt the step response analysis, a well-known control-theoretic method. The adoption includes replacing the human operator (or master) with a controller with known characteristics and analyzing its response to slave side step disturbances. The resulting step response curves demonstrate that the *Quality of Control* (QoC) metric is sensitive to control loop instabilities and serves as a good indicator of cybersickness experienced by human operators. We demonstrate the efficacy of the proposed methodology and metric through experiments on a TCPS testbed. The experiments include assessing the suitability of several access technologies, intercontinental links, network topologies, network traffic conditions and testbed configurations. Further, we validate our claim of using QoC to predict and quantify cybersickness through experiments on a teleoperation setup built using Mininet and VREP.

I. INTRODUCTION

A Teleoperation system consists of a human operator maneuvering a remote slave robot known as teleoperator over a network. The network transports the operator-side kinematic command signals to the teleoperator and provides the operator with audio, video, and/or haptic feedback from the remote-side. In existing teleoperation systems such as in telesurgery, due to significant end-end latency and reliability issues in both networking and non-networking components, the operator, i.e., the surgeon is forced to restrict his/her hand speed when he/she performs remote surgical procedures such as knot-typing, needle-passing, and/or suturing. This restriction in hand speed is required to avoid control loop instability and operator side cybersickness [2]–[4]. Control loop instability occurs when the dynamics of the operator’s hand actions exceed the response time of the teleoperation system. Instability in control loops can cause slave robots to go out of synchronization with the operator’s hand movements, which can lead to disastrous consequences in critical applications. Cybersickness occurs when there is a significant noticeable delay in the operator receiving feedback in response to his/her actions. Cybersickness can result in general discomforts such as eye strain, headache, nausea, and fatigue and deter human operators from prolonged use of the teleoperation system [5].

More recently, researchers have envisioned combining tactile internet, a network architecture characterized by sub-millisecond latency and very high packet reliability (99.999%), with advanced motion tracking hardware and high-speed robotics. This could help realizing teleoperation systems that do not impose restrictions on human hand speed [2], [3], [6]. We refer to these prospective teleoperation systems as Tactile Cyber-Physical Systems (TCPS). TCPS are envisioned to have applications in several domains where human skillset delivery is paramount, as in automotive, education, healthcare and VR/AR sectors. Realizing tactile internet where end-to-end latency and reliability are within the prescribed limits is an important part. We think, however, that significant research concerning the design and evaluation is also an equally important part for building non-networking components such as hardware and its response, speed of algorithms and protocols that accompany a TCPS application.

In this paper, we formalize and investigate the evaluation part of TCPS research. A comprehensive evaluation method is necessary to assess and compare different TCPS implementations and to make objective decisions on the components to use for building TCPS. An evaluation method catering to these needs is still non-existent, and therefore, there is an immediate need to develop one [7], [8]. Towards designing an ideal evaluation method catering to TCPS needs, we propose the following objectives.

- Cybersickness and control loop quality are the two main concerns in TCPS. To ensure that they do not affect TCPS implementations, we must capture these effects early in the TCPS design cycle.
- The experiments constituting TCPS evaluation should be oblivious to the intended application. Additionally, the experimental results should be reproducible and free from subjective errors.
- The experimental results should be captured by a single metric that has a physical significance. This is necessary to judge the effect of different uncorrelated variables on the planned TCPS application.

A. Related Work

Given the nature of TCPS with humans in the loop, an evaluation metric should have the ability to capture bidirectional end-to-end performance. However, in the current literature, TCPS evaluation is done using Quality of Service (QoS) metrics or by subjective methods that employ human operators [9]–[15]. These metrics use several QoS parameters such as latency, jitter, and packet drops, mostly limited to unidirectional end-to-end performance. In the context of TCPS, these metrics have limited utility in checking if an implementation can meet a given specification because these metrics do not relate the quality of the operator’s experience with his/her dynamics. Certain latency and jitter may suit a TCPS with slow operator movement, but may not be adequate for another TCPS with faster operator movement. For instance, it is difficult to arrive at the right combination of these metrics that would result in stable control loops or reduced cybersickness. Thus it is difficult to use them for comparing the performance of different TCPS implementations.

Subjective evaluation methods assess responses from a large number of human operators to formulate a meaningful metric. This metric can be either subjective [9]–[12] or objective [13]–[15]. In either case, subjective evaluation methods are time-consuming, prone to errors and application-specific, and fail to account for operator dynamics as discussed earlier. Importantly, subjective methods cannot truly assess the TCPS control loop quality. For instance, a human operator assigned to evaluate the TCPS may not recognize if the system implementation has low levels of instabilities such as minor overshoots, minor oscillations or minor steady-state errors due to his/her limited sensory perceptions. Low levels of instabilities may be acceptable for non-critical applications. However, for critical applications like telesurgery, even low levels of instabilities can cause injuries to the remote-side patients.¹

B. Key Contributions

- *Evaluation Methodology*: The evaluation method for TCPS has to be generic and objective. For this, we adopt the step response method, a classic control-theoretic method for analyzing the quality of closed-loop systems. In our work, we leverage this method for TCPS by framing an objective evaluation methodology around a typical TCPS implementation. This is accomplished by replacing the human operator with a controller with known characteristics and analyzing its response to slave side step changes. We had introduced this framework to characterize control loop quality of TCPS in [16]. However, this work is the first attempt to use the step response method for evaluating TCPS.
- *Quality of Control*: In the quest for an index to grade TCPS, we propose the metric *Quality of Control*(QoC). QoC is designed to capture the effect of different QoS parameters on the TCPS application. We can, therefore, use QoC as a one-stop metric to grade different TCPS implementations. Being based on the step response method, QoC inherently takes into account the stability of the TCPS control loop. Further, the relation we deduce between QoC and the maximum allowed hand speed of a human operator helps in the design of TCPS free from cybersickness. This relation also associates a physical significance to the metric.

C. Outline

We organize this paper as follows: In Section II, we propose an evaluation model for TCPS. From the different control loops in TCPS, we identify the critical control loops to avoid cybersickness and control loop instability. We propose that the quality of these critical control loops is an indicator of TCPS quality. Section III describes evaluation methodologies to assess the quality of the critical control loops. In Section IV, we propose the QoC metric and explain how to determine QoC from step response experiments. Section V describes the relation between QoC and the maximum allowed operator hand speed (to avoid cybersickness). In Section VI, we detail several notions of QoC in real-time control literature and how they are different from our QoC. In Section VII, we introduce QoC performance curves and their use. We describe the evaluation of QoC in Section VIII and conclude the paper in Section IX.

II. EVALUATION MODEL

A typical TCPS can have multiple control loops, as shown in Figure 1. The control loops differ in their feedback modality. For instance, in the control loop *kinematic-video*, the feedback is video. Similarly, for the control loops *kinematic-audio* and *kinematic-haptic*, the feedbacks are audio and haptic respectively. In all these cases, the feedback is in response to the same kinematic commands from the human operator. Here, the presence of a human operator warrants that these control loops adhere to the stringent QoS specifications, in particular concerning their Round Trip Times (RTT). This is to save the operator from cybersickness and ensure control loop stability.

Let us now discuss the RTT requirements for different TCPS control loops. We also identify the control loops that have the most stringent RTT requirement. We call these *the critical control loops* and propose that the quality of these loop be used to benchmark the TCPS.

¹Note that when instability occurs, we will see its effects at both the operator side manipulator and the remote side robot.

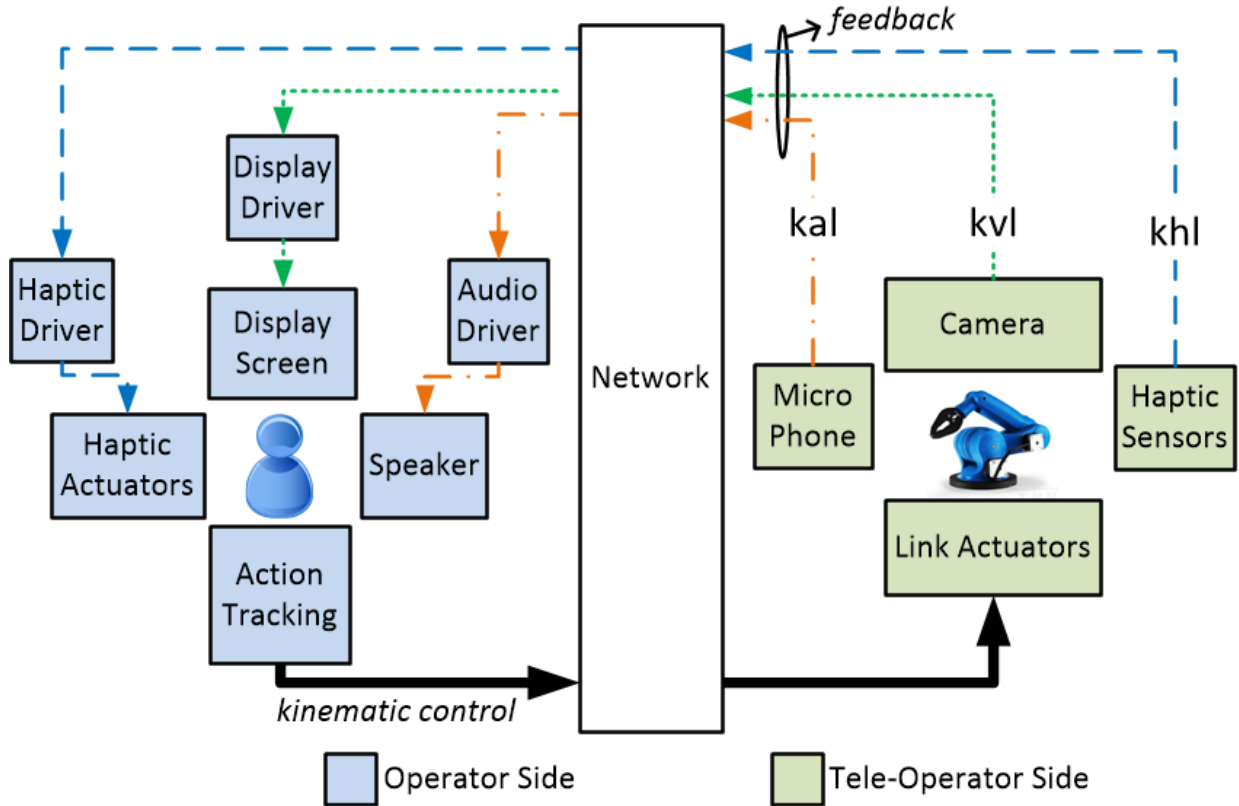


Fig. 1: Functional blocks and control loops in a typical TCPS. (1) kinematic-audio loop (*kal*), (2) kinematic-video loop (*kvl*), and (3) kinematic-haptic loop (*khl*) control loops are shown.

A. Cybersickness

Cybersickness to humans occurs as a result of conflict between different sensory systems. The conflict arises when different sensory systems perceive the occurrence of the same event at noticeably distinct times. In TCPS, cybersickness may result from the asynchronous arrival of different feedback modalities at the operator side in response to the same kinematic commands.

We derive the maximum permissible feedback latencies (or maximum allowed RTTs) for different feedback modalities to avoid cybersickness. These latencies determine the RTT specification of the corresponding TCPS control loops. Note that in a TCPS, delays incurred by both networking and non-networking components contribute to RTT of its control loops.

We begin by observing in Table I the maximum permissible synchronization errors allowed for audio and haptic streams relative to video.² Note that the maximum permissible synchronization errors can be either positive or negative depending on whether the audio and haptic streams arrive after or ahead of the video. However, for TCPS, these streams arriving ahead of the video are not a cause of concern. Hence, we do not account for negative values of synchronization errors.

TABLE I: Maximum permissible *+ve* synchronization errors of different media streams relative to video [17], [18].

| Media Streams | Max Permissible <i>+ve</i> Sync Error Relative to Video |
|---------------|---|
| audio | 45ms |
| haptic | 125ms |

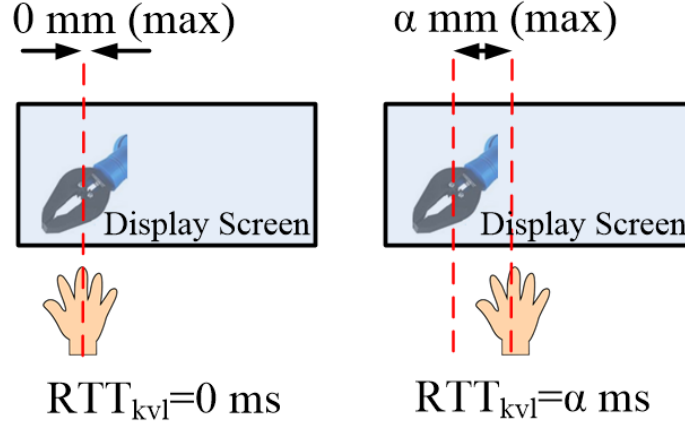
We now derive the maximum permissible feedback latencies (or, maximum allowed RTTs of the corresponding control loops) using these maximum permissible synchronization errors. We show the results in Table II. We assume that the display screen at the operator end shows the actual size of the remote field.

When there is a delay in video feedback, the operator will see a lack of synchronization between the movement of his/her hand and the remote robotic arm displayed on the screen. A typical human operator can move his/her hands at a maximum speed of $1mm/ms$. Moreover, he/she can visually distinguish differences greater than or equal to $1mm$. Therefore, to avoid $1mm$ or larger differences in positions of the operator's hand and the robotic arm displayed on the screen, the maximum

²We consider a TCPS use case where audio and video are streamed independently of each other, unlike the case with streaming methods like MPEG.

TABLE II: RTT specification for TCPS control loops.

| Feedback Modality | Control Loop Specification |
|-------------------|----------------------------|
| video | $RTT_{kvl} \leq 1ms$ |
| audio | $RTT_{kal} \leq 46ms$ |
| haptic | $RTT_{khl} \leq 126ms$ |

Fig. 2: The error between the operator's hand and robotic arm displayed on the screen for a hand speed of $1mm/ms$.

permissible delay for the video feedback is required to be $1ms$. This restricts the RTT of *kinematic-video* loop, RTT_{kvl} , to be less than or equal to $1ms$ [2] (See Figure 2 (a)).³

When the operator moves his/her hand, he/she may expect to hear the sound from the remote environment (e.g. sound of the moving motor joints of the remote side robot or sound of the robot hitting a target) within a specific time limit. If the delay in audio feedback is more than this limit, the operator will find a lack of synchronization between the movement of his/her hand and the audio response. This will also result in cybersickness. We compute the maximum permissible latency for the audio feedback by adding the maximum permissible latency for the video feedback and the maximum permissible *ve* synchronization error of audio relative to the video stream. We thus get the maximum permissible RTT_{kal} to be $46ms$.

Following similar reasoning, we find the maximum permissible latency of the haptic feedback to $126ms$. This restricts RTT_{khl} to $126ms$.

B. Control Loop Instability

As already explained, to avoid cybersickness, the RTT requirement on the *kinematic-haptic* loop is much higher than the requirement on the *kinematic-video* loop. Thus, towards avoiding cybersickness, the *kinematic-haptic* loop is not critical. However, in TCPS where haptic feedback exists in the form of kinesthetic feedback⁴, RTT of the *kinematic-haptic* loop, RTT_{khl} , becomes critical as follows.

In teleoperation systems with kinesthetic feedback, the operator experiences the haptic property (e.g. stiffness) of objects in the remote environment by commanding the teleoperator to tap the surface of these objects at different tapping velocities and sensing the feedback forces through the operator side manipulator [20]. For instance, to differentiate a hard material from a soft material, the operator taps the surface at a higher velocity. At a higher tapping velocity, the force feedback felt by the operator from a hard material will be higher in comparison to a soft material. In TCPS with kinesthetic feedback, to support for the maximum tapping velocity of a typical human operator and thereby enable the operator to differentiate materials of wide stiffness range, the RTT of the *kinematic-haptic* loop, RTT_{khl} is required to be less than $1ms$ [7]. RTT higher than $1ms$ implies that the operator has to restrict his tapping velocity and thus limit his/her ability to differentiate materials of higher stiffness. However, if tapping velocity is not restricted, depending on the stiffness of the material, the *kinematic-haptic* loop may go unstable. This results in high-frequency oscillations in the operator side manipulator and remote side robot.

Unlike in *kinematic-audio* and *kinematic-video* loops, control loop instability can occur in the *kinematic-haptic* loop due to the existence of fast-acting local control loops at the operator and teleoperator sides. These local control loops close the

³Observe that if we restrict the human operator's maximum hand speed to v m/s, RTT_{kvl} can be allowed to be up to $1/v$ ms. Furthermore, if the display screen at the operator's end shows a zoomed out picture of the remote field (say a zoom factor $\alpha < 1$), then even with a maximum hand speed of $1m/s$ and RTT of $1ms$, the synchronization error seen by the operator will be less than α mm. In this case, RTT_{kvl} could be allowed to be larger.

⁴Haptic feedback is of two types, kinesthetic and tactile. Kinesthetic feedback provides information about the stiffness of materials, while tactile feedback provides information concerning the texture and friction of material surfaces. We sense kinesthetic feedback through our muscles, joints and tendons while we sense the tactile feedback through the mechanoreceptors of our skin [19].

global *kinematic-haptic* control loop detouring the human operator (see Figure 3). In regular operation, the local control loops are meant to synchronize both the position and force variables between the operator and the teleoperator sides. However, at higher RTTs, higher tapping velocities and in the presence of stiff materials, they assist in the generation of positive feedback destabilizing the global control loop [20], [21].

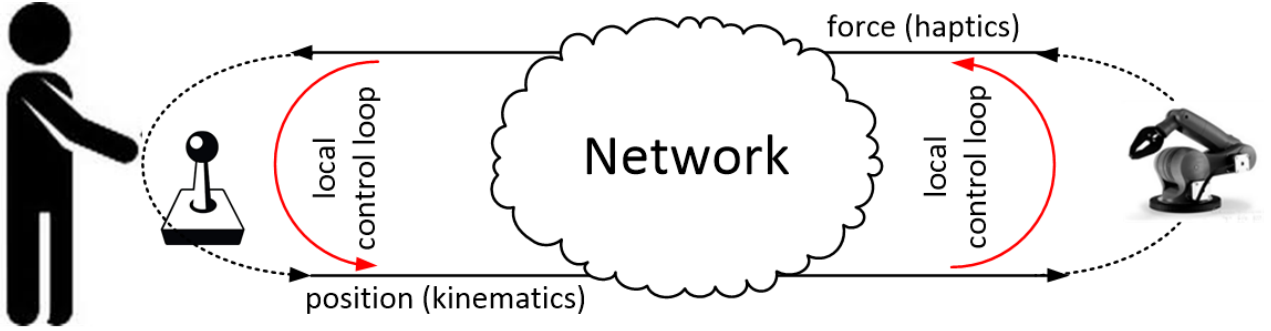


Fig. 3: Presence of fast-acting local control loops in a TCPS with kinesthetic feedback [22].

C. Control Loop for Evaluation

We propose to benchmark a TCPS by evaluating the quality of its critical control loop, the one with the most stringent RTT requirement. We have seen that both *kinematic-video* and *kinematic-haptic* loops are critical loops for avoiding cybersickness and control loop instability, respectively. We propose evaluating one of these loops, depending on which loop is critical for a given TCPS application. In case, if both these loops are equally critical, we propose to evaluate both.

In Table III, we list these possible cases and corresponding possible TCPS scenarios. The occurrence of cybersickness is prominent, i.e., RTT_{kvl} is more critical when the operator hand speed is high. The occurrence of control loop instability is prominent, i.e., RTT_{khl} is more critical when the stiffness of the remote-side object is high for medium and high hand speeds.

TABLE III: Criticality of control loops for different TCPS scenario's.

| | RTT_{kvl} | RTT_{khl} | Sample Scenario |
|--------|-------------|-------------|--|
| Case-1 | ✓ | ✓ | Hand Speed = High Object Stiffness = High |
| Case-2 | ✓ | - | Hand Speed = High Object Stiffness = Low |
| Case-3 | - | ✓ | Hand Speed = Medium Object Stiffness = High |

III. EVALUATION METHODOLOGY

For evaluating TCPS, we use the step response method, a classic control-theoretic method for assessing the quality of closed-loop systems. We leverage this method for TCPS by replacing the human operator with a known Proportional Integral (PI) controller and analyzing its response to the slave side step changes. In this section, we first describe the components of the TCPS testbed implemented in our lab [16]. We then describe how to conduct step response experiments using this testbed in both haptic and non-haptic settings to evaluate *kinematic-haptic* and *kinematic-video* loops, respectively.

A. Component Level Design of the Testbed

The component level design of the testbed is shown in Figure 4.

- *operator* is the human operator or an embedded controller; *tele-operator* is the remote side slave device being controlled.
- *ms embsys* is the master side embedded system which houses sensors, actuators, and algorithms to capture the kinematic motions of the operator, to display audio and video, and to apply haptic feedback to the operator. *ss embsys* is the slave side embedded system that houses sensors, actuators, and algorithms for driving the slave side robot and for capturing the remote audio, video, and haptic signal.
- *ms com* is the master side communication component that connects *ms embsys* to the network; *ss com* is the slave side counterpart which connects *ss embsys* to the network.
- *srv* is the computer for offloading various TCPS algorithms in sensing, actuation, coding, and compression.
- *emu* is the optional emulator used to interconnect the testbed components. The emulator replaces a real physical network. We use ns-3 and Mininet to build this emulator [23], [24].

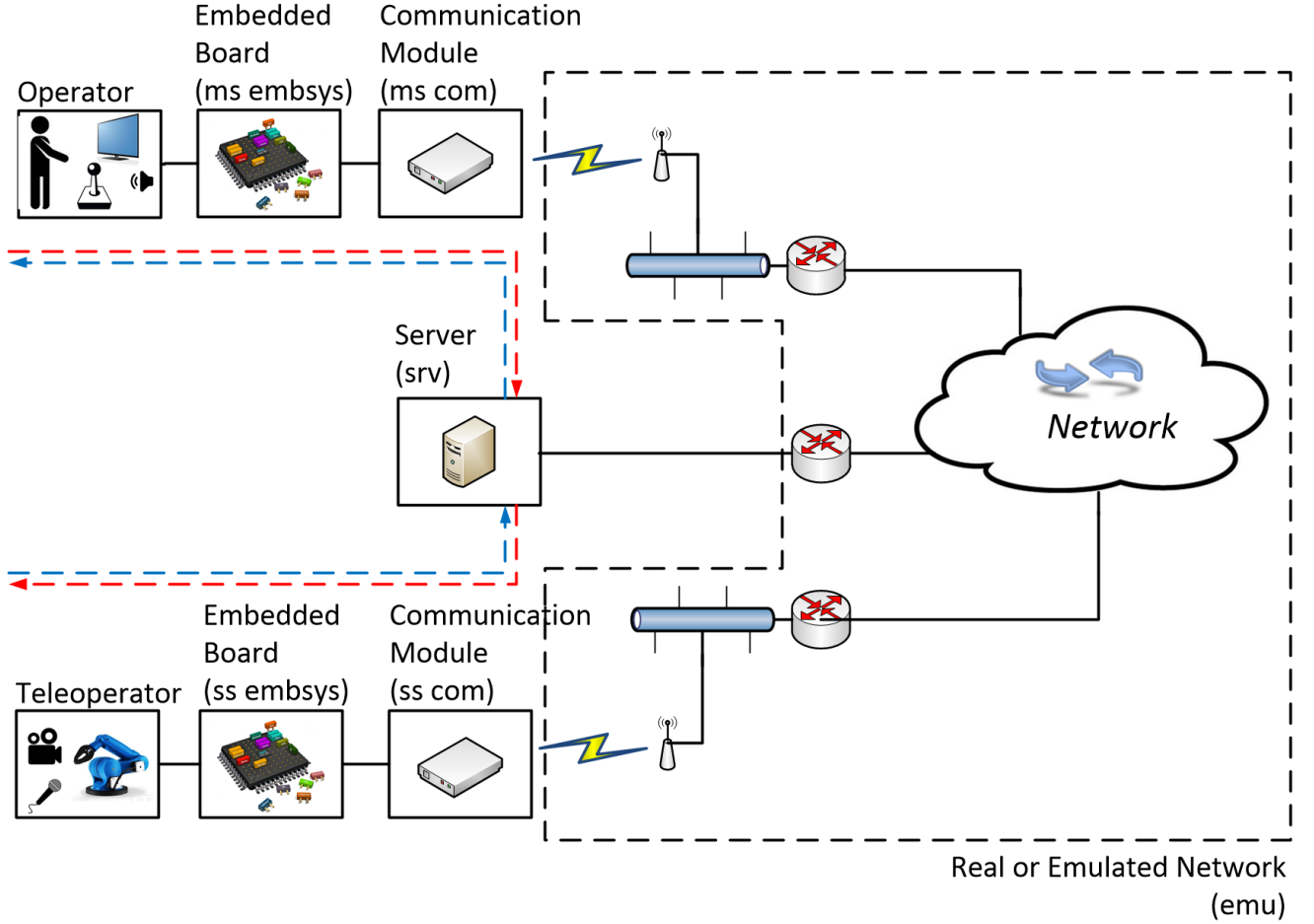


Fig. 4: Component level design of the testbed with forward and backward data flow paths marked [16].

B. Evaluation Framework in a Haptic Setting

Evaluating the *kinematic-haptic* loop helps in quantifying control loop instability in a TCPS. For evaluating the *kinematic-haptic* loop, we propose the evaluation framework in Figure 5. To develop this, we use the testbed in Figure 4 and replace the operator with a PI controller. At the teleoperator side of the testbed, we place a robotic arm with a haptic sensor mounted to its end effector. The haptic sensor detects pressure when the end effector of the robotic arm comes in contact with the material surface. In the step response experiment, we use the PI controller to move the robotic arm along the X-axis and to apply constant pressure of P_{ref} on the material surface along its Y-axis. When the robotic arm crosses the transition point separating the hard and the soft materials, the pressure abruptly drops from P_{ref} to P_{ref}/k_2 , simulating a step-change in the haptic domain. Here k_2 is a constant and is dependent on the characteristics of the materials in use.

The haptic sensor detects this change in pressure and communicates the new pressure to the operator side PI controller. The PI controller uses this data to compute a new y -coordinate of the robotic arm and communicates it back to the teleoperator side to take action. The intent here is to adjust y to increase the applied pressure and correct the haptic step change.

Figure 6 shows a sample haptic step response curve expected from the experiment. The curve resembles the classic step response curve in control system with its quality determined by certain rise time, overshoot, undershoot, settling time, and steady-state error. The quality of this curve directly indicates the quality of the *kinematic-haptic* loop, which in turn indicates the quality of the TCPS under test. In our work, we define *rise time* as $t_r = t_2 - t_0 = t_d + t_2 - t_1$ where,

- 1) t_0 is the time at which the pressure drops to $P_{ref}/k_2 + 0.1(P_{ref} - P_{ref}/k_2)$ (due to step change).
- 2) t_1 is the time at which the pressure rises back to $P_{ref}/k_2 + 0.1(P_{ref} - P_{ref}/k_2)$.
- 3) t_2 is the time at which the step response reaches $P_{ref}/k_2 + 0.9(P_{ref} - P_{ref}/k_2)$.

We define *overshoot* as the peak percentage fluctuation in the step response relative to $(P_{ref} - P_{ref}/k_2)$. Both the rise time and overshoot are affected by the characteristics of the TCPS components and the network.

a) *Operator Side Implementation*: We describe the implementation of the PI controller using the code snippet in Figure 7. Here in every loop, the x coordinate of the robotic arm is incremented by $1cm$. The parameter Δ is the loop wait time used for tuning the responsiveness of the controller and also the stability of the system. A controller using smaller Δ can potentially

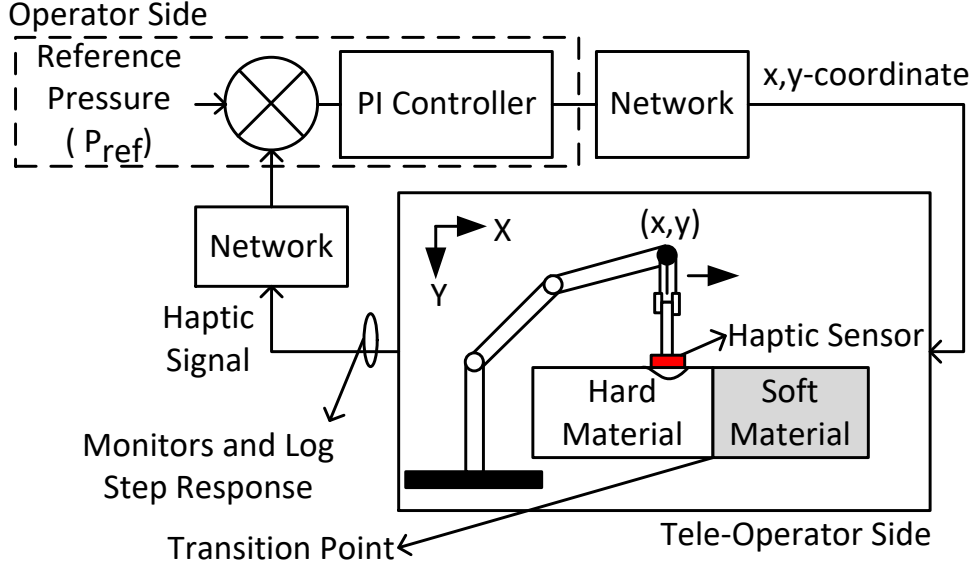


Fig. 5: Evaluation framework

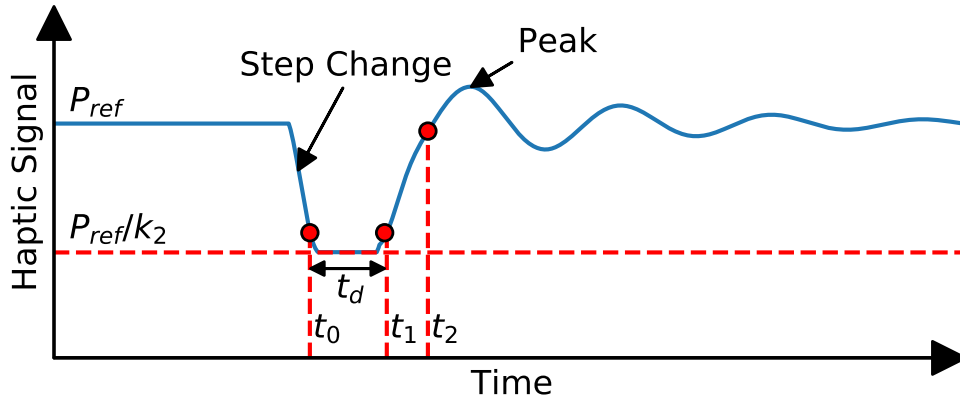


Fig. 6: Sample haptic step response curve. Haptic signal at time instants t_0 , t_1 , and t_2 are marked using red dots.

respond faster to the haptic signal, and therefore lead to smaller rise times. However, setting a very small Δ can potentially result in overshoots and oscillations in the step response curve. In Figure 7, k_p is the PI controller constant.

b) Tele-Operator Side Implementation: In the evaluation framework in Figure 5, we use a robot and a force sensor to simulate and measure the haptic step change. This implementation is useful if, in the TCPS evaluation, we desire to account for the characteristics of the robot and the force sensor. Often we are not interested in accounting for the robot's or sensor's physical limitations (e.g. when we want to evaluate the TCPS communication network). In such cases, we replace the teleoperator side with a code snippet, as shown in Figure 8. In this code snippet, we have used k_1 as the conversion constant to translate y to pressure. The change in pressure from $k_1 y$ to $k_1 y/k_2$ is simulated at $x = X/2$ cm (we choose $X = 100$ in our experiments).

C. Evaluation Framework in a Non-Haptic Setting

Evaluating *kinematic-video* loop of a TCPS helps in determining V_{max} , the maximum operator hand speed the TCPS can support to avoid cybersickness. For evaluating the *kinematic-video* loop, we cannot use the evaluation framework in Figure 5 as it simulates step change in the non-existing haptic domain. In Figure 9, we propose a modified evaluation framework. We use the testbed in Figure 4 and replace the operator using a PI controller with controller constant, k_p , and loop wait time parameter Δ . At the teleoperator side of the testbed, we place a robotic arm with a video camera to detect the y -coordinate of the robot end-effector.

```

OperatorSide ():
  initialize coordinates [ $x = 0, y = 0$ ]
  while ( $x < X_{cm}$ ):
    send robot coordinates  $x$  and  $y$ 
    wait for  $\Delta$  seconds
    if (haptic signal available):
      receive and store in variable  $P$ 
    else:
      store old haptic signal in  $P$ 
    find  $error = P_{ref} - P$ 
    compute  $y = y + k_p \times error$ 
    increment  $x$  by  $1cm$ 

```

Fig. 7: PI controller implementation.

```

TeleOperatorSide ():
  while (true):
    wait to receive coordinates  $x$  and  $y$ 
    if ( $x < X/2$ ):
      set haptic signal to  $k_1y$ 
    if ( $x \geq X/2$ ):
      set haptic signal to  $k_1y/k_2$ 
    send haptic signal to operator side
    log haptic signal to file

```

Fig. 8: Simulating haptic step change at the tele-operator side.

In the step response experiment, we use the PI controller to always maintain a constant y -coordinate, Y_{ref} , for the robotic arm. The PI controller in every control loop (i.e., after every Δ interval of time), increments, and send an epoch variable, n , to the teleoperator side. The PI controller initializes n to 1 at the start of the experiment. At the teleoperator side, n is used to set the value of k_2 . The teleoperator initializes k_2 to 1 at the start of the experiment and is set to a higher value when n is ≥ 50 . This simulates a step-change in the robot y -coordinate, y' , at $n = 50$. The video camera at the teleoperator side detects the change in y -coordinate of the robot and communicates this new y -coordinate to the operator side PI controller. The PI controller uses this data to compute y , a new y -coordinate for the robotic arm and communicates it back to the teleoperator side to take action. The intent here is to adjust y to correct the step-change in y' . The parameters of the resultant step response curve, i.e., the plot of y' , is similar in shape to Figure 6 and is used to evaluate the quality of the *kinematic-video* loop and thus the TCPS under test.

As for the evaluation framework in Figure 5, here also, we can replace the robot and the video camera with a code snippet if accounting the overhead of these components is not desired in evaluation.

Discussion: In the evaluation framework, we discount the characteristics introduced by the display driver block. This is because display driver overheads are generally deterministic and known apriori, and their impact can be theoretically determined.

IV. QUALITY OF CONTROL

In this section, we first describe how to arrive at the optimum value of Δ , denoted as Δ_{opt} . We then describe how to determine the parameters P_{ref} , k_1 , k_2 and k_p of the evaluation framework. We then describe QoC, the evaluation metric we propose for TCPS. For descriptions, we consider step response curves from the evaluation framework proposed for evaluating the *kinematic-haptic* loop. Note that the methods we describe here are also valid for the evaluation framework proposed for a non-haptic setting, i.e., for evaluating the *kinematic-video* loop. In the following, we write rise time as $t_r(\Delta)$ to show its dependence on Δ .

A. Determining Δ_{opt}

The step response curve extracted from the evaluation setup depends on the characteristics of the TCPS under test and also on Δ . For any given TCPS, different values of Δ lead to different step response curves. If Δ is very small, the resulting step response curve can have oscillations and overshoots. As we increase Δ , the controller's response gets slower, and hence oscillations and overshoots reduce, and the rise time increases. We define a good step response curve to be a response curve in

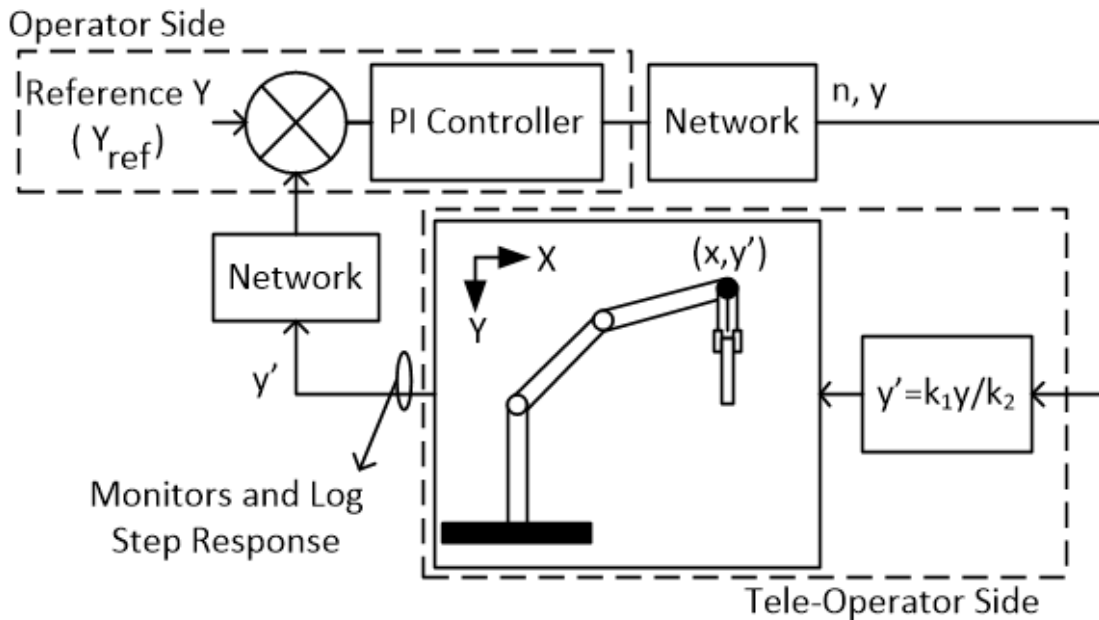


Fig. 9: Evaluation framework for a non-haptic setting.

which the overshoots and steady-state error are within prescribed limits - we set these limits to 20% and 10% respectively in our work⁵. We want to achieve the fastest good response curve, i.e., the good response curve with the least rising time. Accordingly, we should set Δ to the least value that results in a good response curve; we refer to this value as Δ_{opt} . Alternatively stated, $\Delta = \Delta_{opt}$ results in a response curve that has the least rise time among all the response curves with overshoots and steady-state errors within 20% and 10% respectively. In the following, we refer to this good response curve as a Δ_{opt} -curve.

We determine Δ_{opt} through experiment. For the TCPS under test, Figure 10 shows the step response curves for a few values of Δ . Observe that, with 20% and 10% limits, the overshoots and steady-state error for good response curves should be less than 4units and 2units respectively. In particular, peaks of good response curves should be less than 104units. $\Delta = 0.1ms$ and $\Delta = 0.6ms$ yield response curves with peaks exceeding 104units. On the other hand, $\Delta = 0.7ms$ yields the good step response curve with the least rise time. We thus determine $\Delta_{opt} = 0.7ms$. Note that a smaller Δ_{opt} implies a potentially smaller t_r and hence a better quality TCPS.

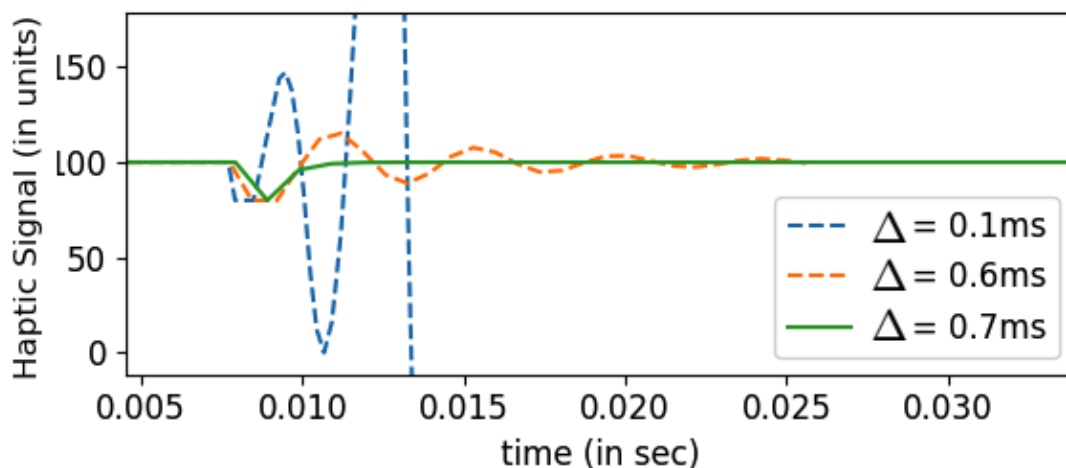


Fig. 10: Step response curves of a sample TCPS for a few values of Δ . Here $P_{ref} = 100$ and $P_{ref}/k_2 = 80$.

⁵In our work, we set limits only on overshoot and steady-state error to identify good step response curves. This is to simplify the classification of step response curves. In practice, we advise setting limits on all step response curve parameters including undershoot and settling time.

B. Design of Evaluation Parameters

For a TCPS with zero packet loss and $RTT < \Delta$, we can deduce a difference equation from the basic PI controller equation as follows. Let y_l be the current y -coordinate of the robot and y_{l+1} be its next y -coordinate determined by the PI controller. Then, for stability and fast convergence of this difference equation, the roots of its characteristic equation in the Z domain, $z - (1 - k_p k_1 / k_2) = 0$, should be within the unit circle and close to the origin.

$$\begin{aligned} y_{l+1} &= y_l + k_p \times error \\ &= y_l + k_p (P_{ref} - P) \\ &= y_l + k_p \left(P_{ref} - \frac{k_1 y_l}{k_2} \right) \\ &= y_l \left(1 - \frac{k_p k_1}{k_2} \right) + k_p P_{ref} \end{aligned}$$

We see from the characteristic equation that P_{ref} does not influence the stability or the convergence speed of the difference equation. Thus we can choose any value for P_{ref} . For ease of design we fix $P_{ref} = 100$ units. The parameter k_2 allows realizing the haptic step. We want to set k_2 to restrict the step signal to 20% of the P_{ref} . This is necessary to maintain the operation of the slave device around its operating point. We thus set $k_2 = 1.25$. Furthermore, we could set $k_p k_1 = k_2 = 1.25$ so that the root of the characteristic equation would be at the origin of the Z -plane. This would ensure that the configuration of the evaluation setup does not mask the characteristics of the TCPS under test, and we also achieve the fastest possible step response. However, this results in an overshoot at the start of the step response experiment (See Figure 11). This is because, initially, when $x < 50$ units the effective value of k_2 is 1 which results in the root of the characteristic equation to be in the left half of the Z -plane. In order to ensure that the root of the characteristic equation is positive all through, we set $k_p k_1 = 1$. In particular, we choose $k_1 = k_p = 1$.

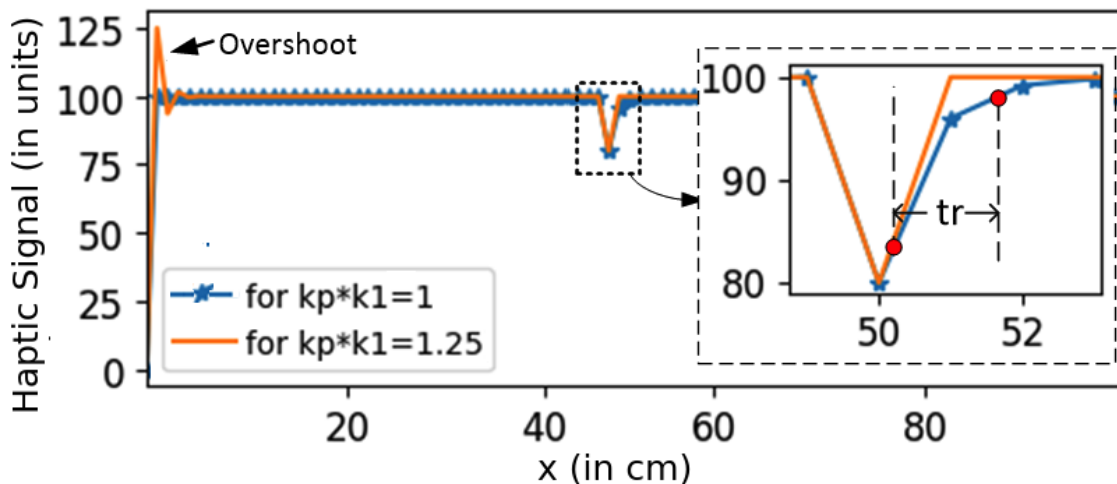


Fig. 11: Haptic step response curve for different $k_p k_1$ settings for a TCPS with zero packet drops and $RTT_{max} < \Delta$. For $k_p k_1 = 1.25$, we see overshoot at the start of the step response experiment.

We do not recommend setting $k_p k_1 < 1$. A lower $k_p k_1$ can increase the response time and can impact the ability of the evaluation methodology to detect packet drops or latency issues commonly observed with the TCPS communication networks. We demonstrate this in Figure 12. We simulate packet drops in the communication network of a TCPS under test. We see that packet drops cause an overshoot when $k_p k_1 = 1$ but do not when $k_p k_1 = 0.6$. Hence we can detect packet drops from overshoot in the former case but cannot detect these in the latter case.

C. Design of Evaluation Metric

To evaluate TCPS, we propose a metric that is an indicator of TCPS control loop quality. We call this metric *Quality of Control (QoC)*. QoC of a TCPS is a relative measure of its quality compared to the quality of an ideal TCPS where an ideal TCPS is one with $1ms$ RTT, zero packet loss and zero jitter. Notice that Δ_{opt} for the ideal TCPS will be equal to its RTT, i.e., $1ms$. Let $t_{r,ideal} \triangleq t_{r,ideal}(1ms)$ be the rise time of the corresponding Δ_{opt} curve. We then define QoC for the TCPS under test as,

$$QoC = \log_{10} \left(\frac{t_{r,ideal}}{t_r(\Delta_{opt})} \right) \quad (1)$$

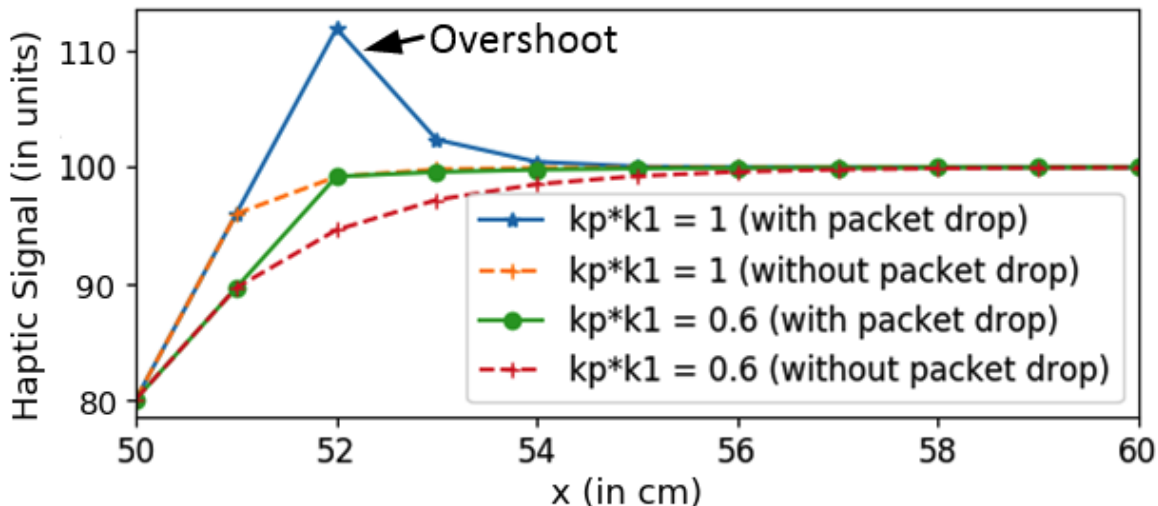


Fig. 12: Haptic step response curve (zoomed-in) for different $k_p k_1$ settings; with and without packet drops.

Where, $t_r(\Delta_{opt})$ is the rise time of the Δ_{opt} -curve of the TCPS under test. We use \log_{10} for the convenience of representing t_r ratio. We expect rise time ratio in (1) to assume a wide range as the latencies associated with TCPS components (e.g., network latency) can vary widely. This is why we use a logarithmic scale to specify QoC.

We now describe how we compute $t_{r,ideal}$. Observe that $t_{r,ideal}$ depends on k_p and k_1 through their product. We set $k_p k_1 = 1$ as suggested in Section IV-C. From Figure 11, we see that, for an ideal TCPS with $k_p k_1 = 1$, the PI controller takes three loop times ($\approx 3\Delta_{opt} = 3ms$) from $x = 50cm$ to $x = 53cm$ to correct the step change. Also $t_{r,ideal}$ is 1.5 loop times $\approx 1.5ms$.

Observe that QoC of the TCPS under test will be positive if it has $t_r(\Delta_{opt}) < 1.5ms$ and negative if it has $t_r(\Delta_{opt}) > 1.5ms$. The metric intuitively indicates how fast (or slow) the operator can control the teleoperator using the haptic feedback without introducing significant control glitches at the teleoperator side.

Discussion: We have found several notions of quality of control, also referred to as QoC, in real-time control literature [25]–[31]. These definitions of QoC refer to objective metrics used for measuring the performance of generic control systems. QoC in the present work is, however, different from these existing notions in terms of its objective, usefulness and measurement method. We describe these differences in Section VI.

D. Methodology to Determine QoC

The above definition of QoC is on the presumption that each TCPS (for a given k_p, k_1) has an optimal loop wait time, Δ_{opt} . Also, Δ_{opt} , which is a function of TCPS RTT, packet drop rate, etc., can be estimated through a sequence of step response experiments. However, for any TCPS, its RTT, packet drops, etc., may vary with time. Hence, QoC, if measured as defined above, will vary with time. One can define QoC for a TCPS for the worst-case RTT and packet drops, but such a measure will present a pessimistic picture of the system and will be of little consequence in practice. In most of the applications, we want good responses for a prescribed fraction, say g_{spec} , of time. We call g_{spec} the desired goodness percentage. For instance, g_{spec} could be 0.99 for critical applications and smaller for others. Here, we give an alternate characterization of the quality of control as a function of the desired goodness percentage; we call it $\overline{QoC}(g_{spec})$. We also describe a way to measure it in practice.

Recall that Δ_{opt} is the minimum value of Δ that yields a good response. We define $\overline{\Delta_{opt}}(g_{spec})$ to be the minimum Δ that yields a good response curve g_{spec} fraction of time. Note that $\overline{\Delta_{opt}}(g_{spec})$ will be large for a large g_{spec} . We can obtain $\overline{\Delta_{opt}}(g_{spec})$ as follows. We choose a small Δ and run the step response experiment a large number of times, say m times. We determine the fraction of times, say $g \approx (g > 0)$, good response curves are obtained. The parameter m is selected to limit the 95% confidence interval range of g to be within $\pm 5\%$. We now increase or decrease Δ depending on whether g is smaller or larger than g_{spec} and repeat the above experiments until $g = g_{spec}$. The final value of Δ is the desired $\overline{\Delta_{opt}}(g_{spec})$. We define $t_r(\overline{\Delta_{opt}}(g_{spec}))$ to be the average value of t_r over all the good response curves corresponding to $\overline{\Delta_{opt}}(g_{spec})$. Finally, we define,

$$\overline{QoC}(g_{spec}) = \log_{10} \left(\frac{t_{r,ideal}}{t_r(\overline{\Delta_{opt}}(g_{spec}))} \right) \quad (2)$$

E. Factoring in the Effect of Data Packet Size

In the evaluation methodology discussed we use an approximate model for an end-to-end TCPS. We assume there are only one haptic sensor and two degree of freedom for the robot. Here the forward kinematic and backward haptic signal packets are thus limited in size. However, a real TCPS will have a robot with multiple degrees of freedom and an array of haptic sensors which increase the data packet size. The increase in the data packet size can affect the end-to-end system latency, jitter, and packet errors. We thus believe for evaluation, we have to account for the real data packet size. For this, we propose a modified evaluation framework (see Figure 13). We modify the code snippets at the operator and tele-operator side to simulate a defined packet of size B bytes. We do this by appending the haptic and kinematic data packets with random bytes and the corresponding checksum. At the operator and tele-operator side, we accept the packets only upon a matching checksum. This enables us to capture the effects of packet errors in the forward and backward TCPS channels. For evaluating QoC, we set B to match the data packet size of a real-world TCPS.

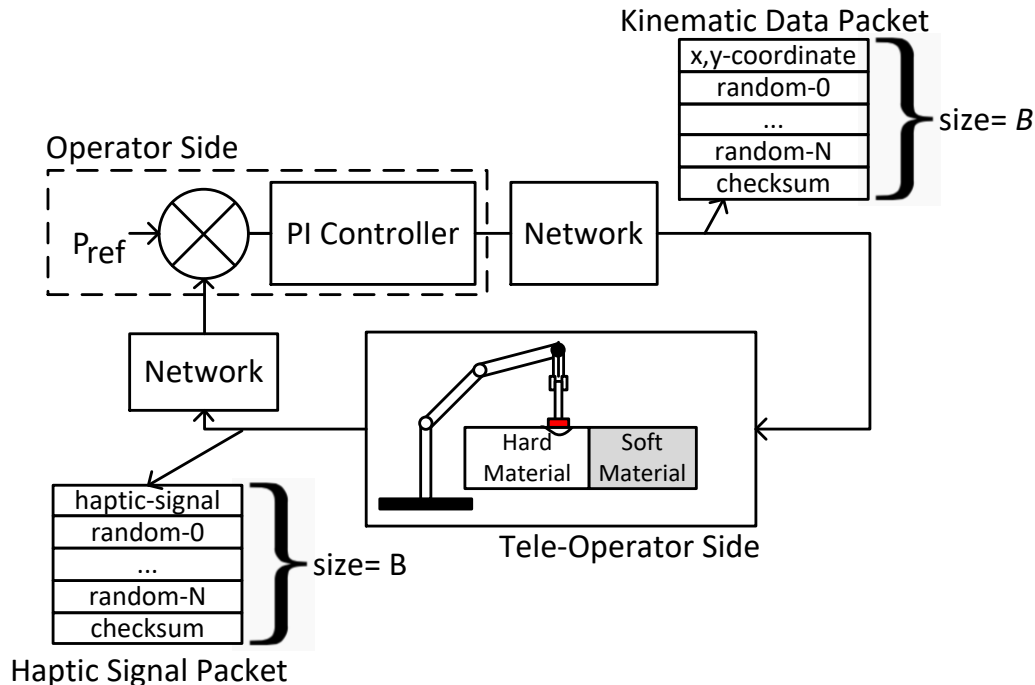


Fig. 13: Evaluation framework to account for variable data packet size.

V. QoC VS. OPERATOR KINEMATICS

For a human operator, the maximum allowed hand speed, V_{max} , to avoid cybersickness is limited by two factors: the natural limit on human hand speed ($1m/s$) and the quality of the TCPS *kinematic-video* loop. The latter is not the limiting factor in an ideal TCPS. More specifically, an ideal TCPS with $RTT = 1ms$ and $\overline{QoC}(1) = 0$ supports $V_{max} = 1m/s$.⁶ A TCPS with lower $\overline{QoC}(g_{spec})$ (for the given g_{spec}) will support smaller hand speeds only, i.e., it will have $V_{max} < 1m/s$. In this section, we first derive the relation between $\overline{QoC}(g_{spec})$ and V_{max} . We then validate this relation through simulation.

1) *Maximum hand speed:* For an ideal TCPS with $RTT = 1ms$ and no packet drop and jitter, the step response graph of robot y -coordinate i.e., plot of y' , and the graph of operator's hand position i.e., plot of y , controlling the y -coordinate of the robotic arm, sampled at every $1ms$, will have the same rise time t_r ; see Figure 14. For the plot, we choose $Y_{ref} = 100mm$ and use δy to represent the change in operator's hand position. This condition (the rise time being the same) prevails in generic TCPS also, provided we use $\Delta \geq \overline{\Delta}_{opt}(g_{spec})$. In the case of a generic TCPS, t_r and δy are replaced with $t_r(\overline{\Delta}_{opt}(g_{spec}))$ and $\delta y(\overline{\Delta}_{opt}(g_{spec}))$, respectively.

We define the maximum allowed operator's hand speed V_{max} as dy/dt . For generic TCPS,

$$V_{max} = \frac{dy}{dt} = \frac{\delta y(\overline{\Delta}_{opt}(g_{spec}))}{t_r(\overline{\Delta}_{opt}(g_{spec}))}. \quad (3)$$

⁶For an ideal TCPS with no randomness, for all g , $\overline{QoC}(g) = QoC = 0$.

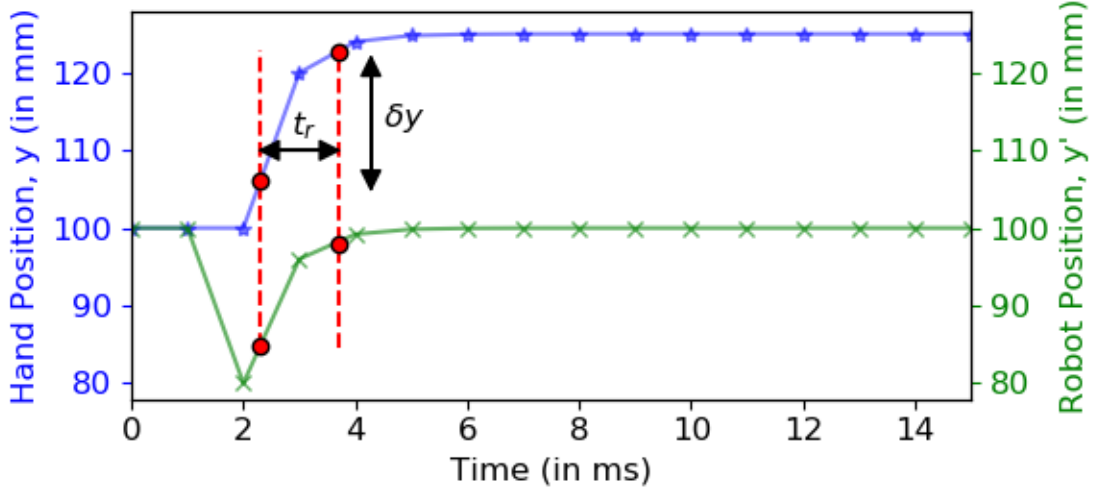


Fig. 14: Step response plots of the operator's hand position, y , and haptic signal for an ideal TCPS with zero packet drop and $RTT_{max} = 1ms$, and for a data sampling interval of $1ms$.

Substituting $t_r(\Delta_{opt})$ from (1) in (3), we get

$$V_{max} = \frac{\delta y(\overline{\Delta_{opt}}(g_{spec}))}{t_{r,ideal}} \times 10^{\overline{QoC}(g_{spec})}. \quad (4)$$

Applying (4) to the ideal TCPS, i.e., substituting $V_{max} = 1m/s$ and $\overline{QoC}(g_{spec}) = 0$, we obtain $\delta y(\overline{\Delta_{opt}}(g_{spec}))/t_{r,ideal} = 1m/s$, a constant. Using this and also noting that V_{max} is limited to $1m/s$, the natural limit on human hand speed, we obtain the following simple relation between V_{max} and $\overline{QoC}(g_{spec})$ in any TCPS. We illustrate this relation in Figure 15.

$$V_{max} = \min\{1, 1 \times 10^{\overline{QoC}(g_{spec})}\}m/s. \quad (5)$$

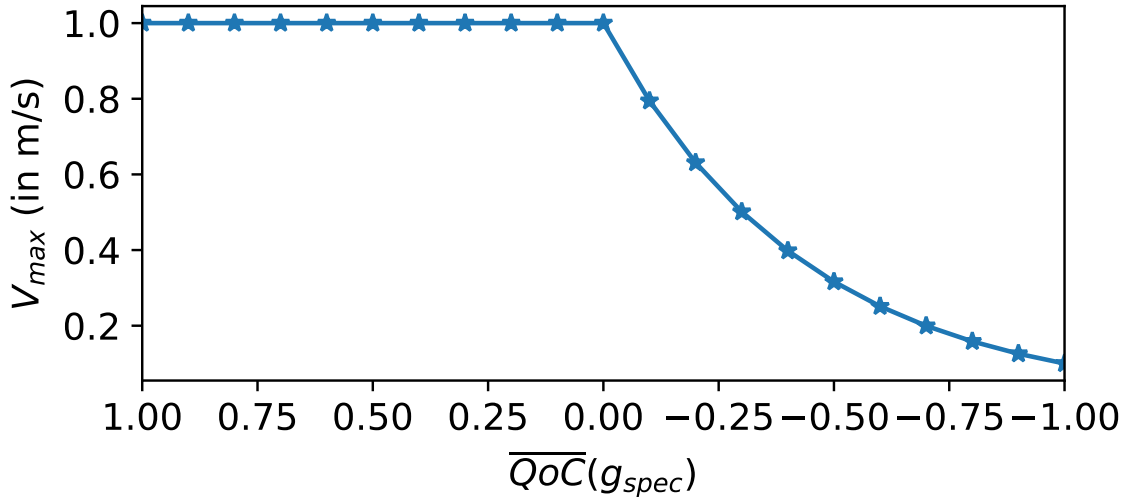
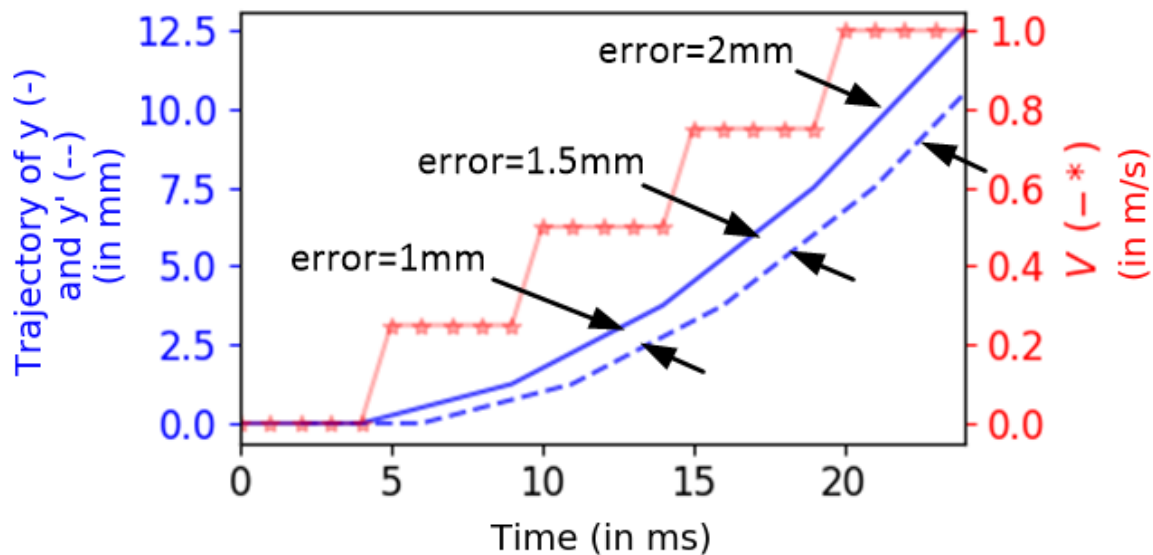


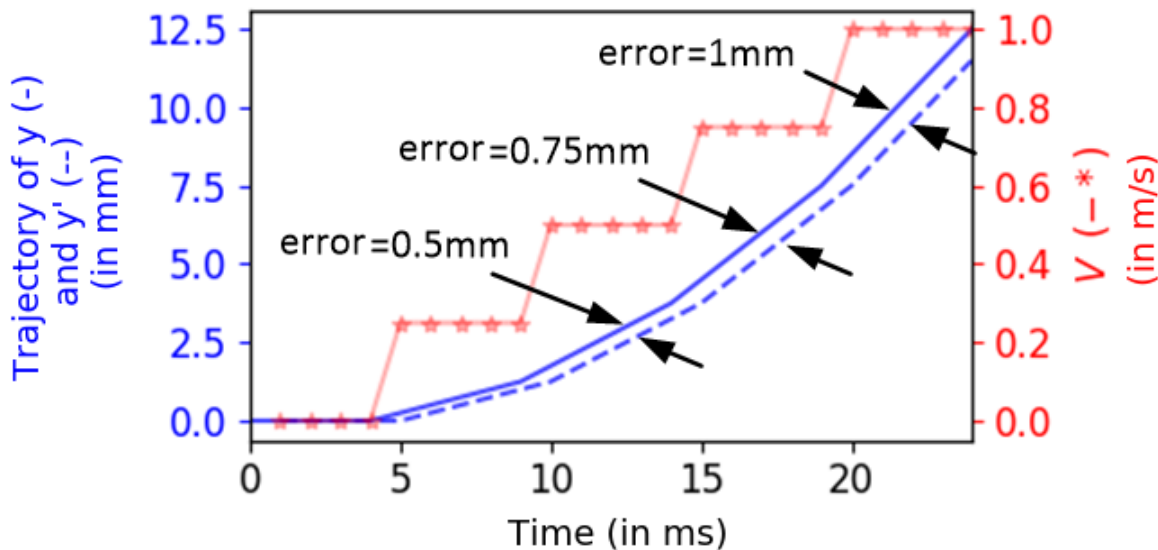
Fig. 15: Graph relating V_{max} and QoC .

2) *Simulation Results:* In any TCPS applications, the human operator is expected to restrict his hand speed to V_{max} a limit posed by the underlying TCPS. If the hand speed exceeds, the operator may experience cybersickness due to visible error ($> 1mm$) between his/her hand position and the robot position seen in the video feedback (see Figure 2). We demonstrate this in Figure 16a and 16b. Here, y represents the operator's hand position and y' represents the robot position displayed on the

operator side screen. For Figure 16a, we consider a TCPS with $\overline{QoC}(1)$ which corresponds to $V_{\max} = 0.5m/s$. As long as the operator maintains his hand speed, V , within $0.5m/s$, the error between y and y' is bounded within $1mm$. This error crosses $1mm$ when V exceeds $0.5m/s$. For Figure 16b, we consider a TCPS with $\overline{QoC}(1) = 0$ which corresponds to $V_{\max} = 1m/s$. Here the error between y and y' remains within $1mm$ up to $V = 1m/s$.



(a) For a TCPS with $\overline{QoC}(1) = -0.3$. Here error exceeds $1mm$ for $V > (V_{\max} = 0.5m/s)$.



(b) For a TCPS with $\overline{QoC}(1) = 0$. Here error remains within $1mm$ upto $V = (V_{\max} = 1m/s)$.

Fig. 16: Plots describing how the error between the operator's hand position, y , and robot position, y' , vary with operator hand speed, V , for TCPS with different QoCs.

VI. QOC IN LITERATURE: DEFINITIONS AND DIFFERENCES

We find that QoC is a term often used in real-time control literature. It refers to objective metrics used for measuring the performance of control systems. Several definitions of $QoCs$ are found in literature [25]–[31]. Broadly, we classify these definitions into two groups depending on the performance measures authors use to determine QoC.

Definition-1: To determine QoC, authors measure the integral of error, e , after simulating a step disturbance in the control loop shown in Figure 17. Authors may use different approaches to measure integral of error like integral of absolute error

TABLE IV: Essential differences between our definition of QoC and QoC definitions in real-time control literature.

| | QoC (Our Definition) | QoC (in Literature) |
|------------------------------|---|--|
| Objective | Evaluates plant (TCPS) performance for a given controller and load. | Evaluates controller performance for a given plant and load. |
| Performance Measure | Rise time of good step response curves. | Time domain integration of step response signals. |
| Physical Significance | Useful in determining V_{max} . | No physical significance. |

(IAE), integral of square error or integral of weighted absolute error. For example, authors in [25], [26] measure IAE to determine QoC as follows.

$$IAE = \int_0^{\infty} |e(t)| dt \quad (6a)$$

$$QoC = \frac{1}{IAE} \quad (6b)$$

Definition-2: To determine QoC, authors measure the quadratic cost, J , instead of integral of error [27]–[31]. Equation(7) represent the generic form of J . u is the input to the plant, s is the plant state variable, and R and Q are weighing inputs. QoC evaluation using J has the advantage that it accounts for both the error and the energy consumed by the controller.

$$J = \frac{1}{2} \int_0^{\infty} Ru(t)^2 + Qs(t)^2 dt. \quad (7)$$

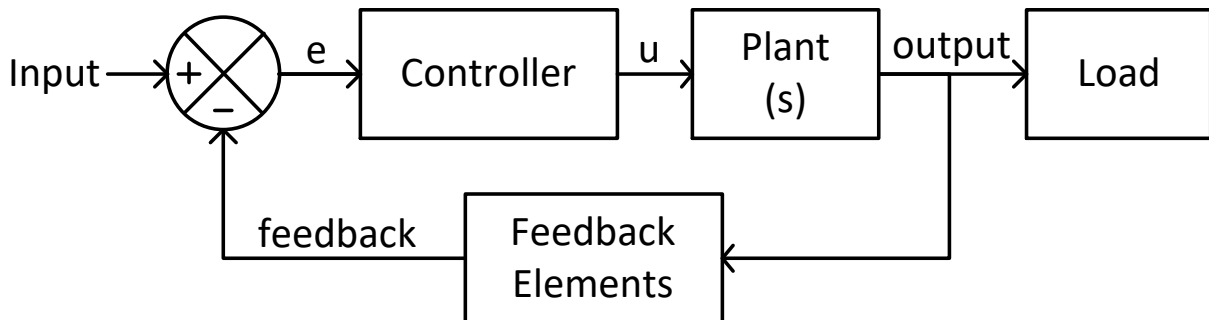


Fig. 17: Block representation of a generic control system.

In Table IV, we list the essential difference between our definition of QoC and QoC definitions in the literature.

- Although QoCs in the literature and QoC presented in our work both measure control performance, their objectives are different. In literature, authors use QoC to assess the quality of the controller for a given plant and a given load. However, we use QoC with the intent of assessing the quality of the plant, i.e. the TCPS. It is for this reason, we fix the controller and the load by fixing k_p , k_1 and k_2 .
- In the literature, authors, determine QoC by time-domain integration of signals (e.g. IAE , J). QoC's in the literature thus cannot comprehend the real dynamics of a control system [25]. For instance, it is possible that two different control systems, one that generates a spiky transient response with a low steady-state error and the other that generates a non-spiky transient response with a high steady-state error, can both yield the same IAE . In generic control systems, this might be acceptable but not for TCPS applications, where the presence of spikes can hamper the remote operation. For this reason, we use $t_r(\Delta_{opt}(g_{spec}))$, the rise time of the tuned step response curves as the performance measure to determine QoC. Recall that tuning of step response curves ensures Δ_{opt} and thus t_r to account for both the transient and steady-state components of the error.
- The performance measures the authors use to determine QoCs in the literature devoids the resultant metric from having a physical significance, i.e., for a TCPS, they cannot comment on the recommended maximum operator hand speed, V_{max} . We determine QoC by measuring the rise time of the tuned good step response curves and describe in Section V how to relate V_{max} and QoC.

VII. QoC PERFORMANCE CURVE

When comparing performance of different TCPS using QoC, we use a common g_{spec} (i.e., $\overline{QoC}(g_{spec})$). Here g_{spec} is specified by the TCPS application. However, when vendors publish QoC for TCPS targeting multiple applications, listing QoC for one g_{spec} is not enough. As a solution, we propose publishing the QoC performance curve for TCPS. The curve illustrates how QoC varies with g_{spec} . In Figure 18, we plot sample QoC performance curves for three different TCPS. From the curves, we conclude the following; (i) for applications that demand $g_{spec} = 0.7$, TCPS-1 has better performance compared to TCPS-2 and TCPS-3 (ii) for applications that demand $g_{spec} = 0.9$, TCPS-2 has the better performance compared to TCPS-1. For this application, we cannot consider TCPS-3 as its QoC for $g_{spec} > 0.8$ is not specified.

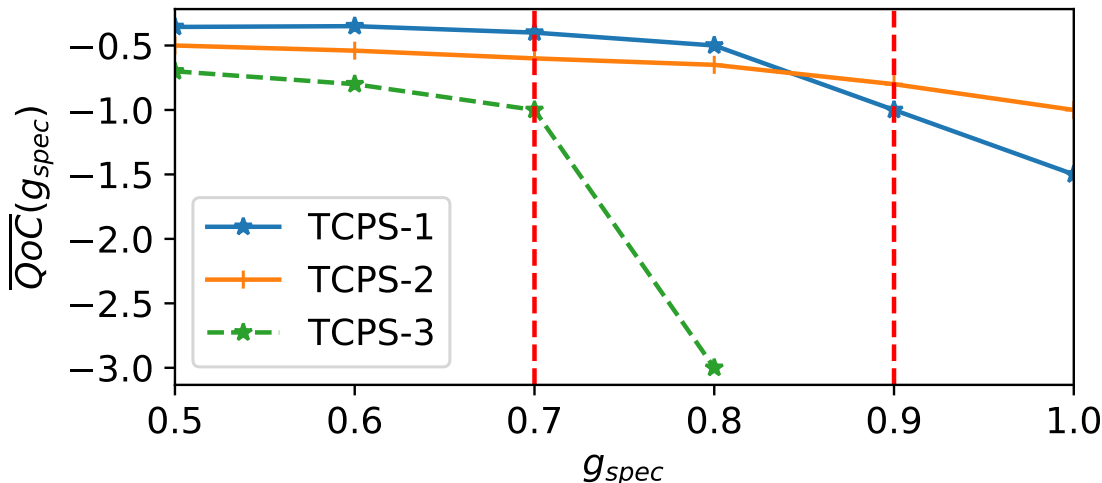


Fig. 18: Sample QoC performance curves for three different TCPS.

VIII. PERFORMANCE EVALUATION

In this section, we demonstrate how to use QoC to evaluate the overhead of a TCPS testbed, evaluate the quality of a TCPS network under different traffic conditions and to validate the effectiveness of QoC in quantifying cybersickness.

A. Evaluating the Testbed Overhead

We determine the overhead introduced by the testbed in Figure 4 in terms of QoC. We find the overhead of the testbed framework without the network emulator to be $\overline{QoC}(0.9) = -0.35$. With network emulator, the overhead increases to $\overline{QoC}(0.9) = -0.92$.

a) Overhead of Testbed Framework: To evaluate the overhead introduced by the testbed framework, we realize the components *ms com*, *srv* and *ss com* in a single desktop PC (Processor: Intel-Core-i5, Core Count: 4, Processor Frequency: 3.4GHz, Memory: 3.7GiB) with $< 10\%$ and $< 20\%$ CPU and RAM utilizations, respectively (see Figure 19). To ensure the results are representative of the testbed overheads alone, (i) we retain minimal code in the testbed components to enable only the needed inter-component communication and (ii) we substitute the teleoperator side using a code snippet that also simulates the step input (to avoid accounting for teleoperator side component overheads). Following the steps (i) and (ii) results in the evaluation frameworks defined for a haptic setting and for a non-haptic setting to appear indistinguishable. i.e., irrespective of which evaluation framework we use, the end QoC will be the same.

We run the experiment to extract the step response curves for different values of Δ . For each Δ , we extract $m = 1000$ step curves. (see Figure 20).

Result: We find $\overline{\Delta_{opt}}(0.9) = 1.9ms$, $t_r(\overline{\Delta_{opt}}(0.9)) = 3.364ms (\pm 0.21\%)$ and $\overline{QoC}(0.9) = -0.35$. The metric indicates that the testbed implemented on the selected desktop PC and OS configuration is inadequate to realize ideal TCPS with $1ms$ RTT. We either have to optimize the socket I/O calls or optimize background processes or replace the hardware. Note that, $QoC < 0$ does not mean that the TCPS implementation is not useful. It means the operator has to restrict his/her maximum hand speed to V_{max} during teleoperation. From (5), $V_{max} = 0.44m/s$.

b) Overhead of Integrating Network Emulator : To understand the overall overhead of the testbed with the network emulator in place, we modify the setup in Figure 19. We evaluate QoC by placing the components *ms com* and *srv* in PC#1, *emu* running the ns-3 code in PC#2 and *ss com* in PC#3 (see Figure 21). The PCs are connected using point-to-point gigabit Ethernet links to interconnect the components, as shown in Figure 4. In ns-3, we emulate an ideal point-to-point link of zero latency, and zero packet drops to ensure the QoC measurement captures the testbed overhead alone and not the effects of any network components in ns-3.

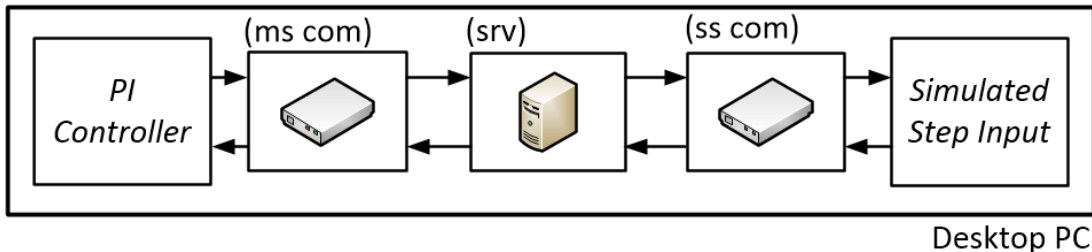
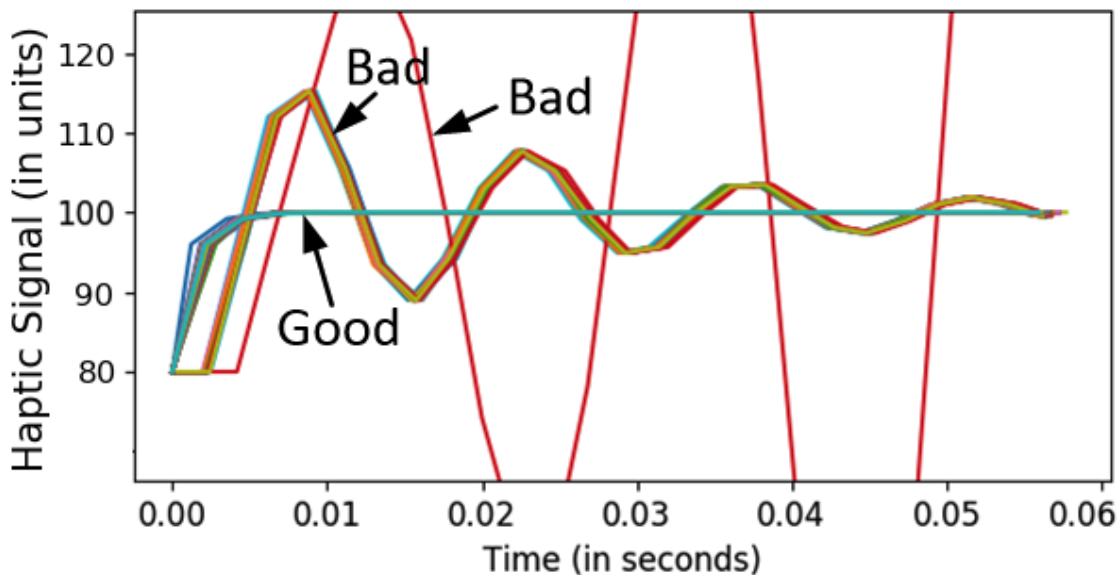
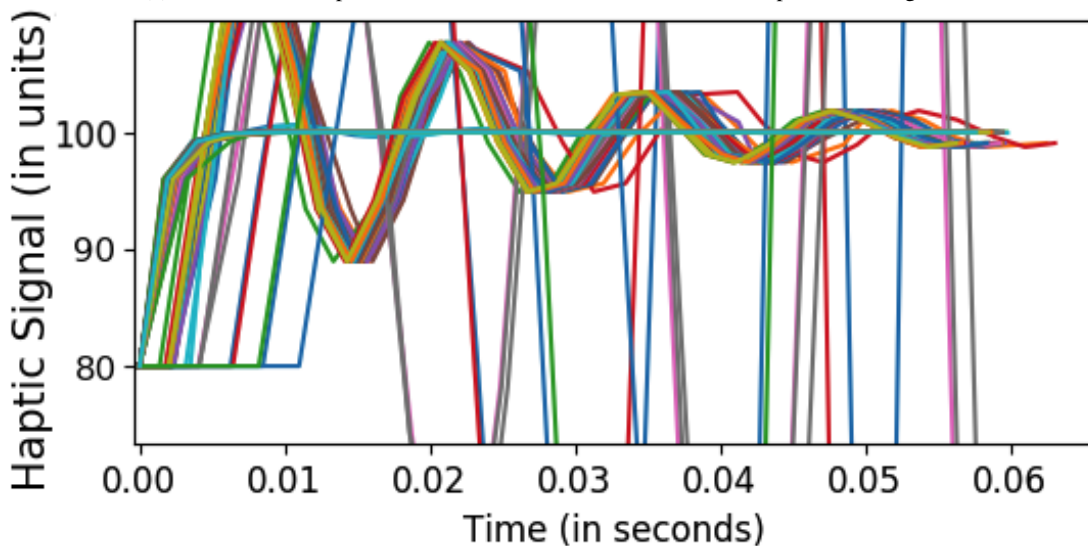


Fig. 19: Setup for evaluating the testbed overhead. Arrows mark the forward kinematic and backward haptic signal flows



(a) Plot of 1000 step curves for $\Delta = 1.9ms$. Here 90.6% of step curves are good.



(b) Plot of 1000 step curves for $\Delta = 1.8ms$. Here 80% of step curves are good..

Fig. 20: Plot of 1000 step curves for two different Δ . We find, $g > 0.9$ only when $\Delta \geq 1.9ms$. Thus we determine $\overline{\Delta}_{opt}(0.9) = 1.9ms$ for a $g_{spec} = 0.9$.

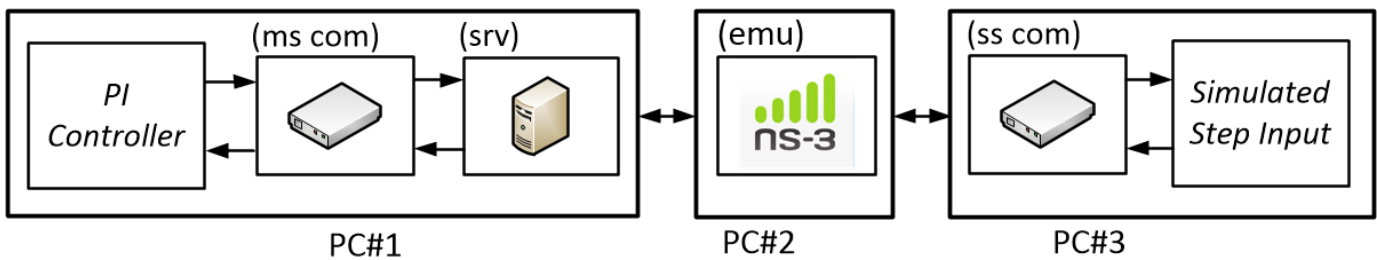


Fig. 21: Setup for evaluating the testbed overhead with network emulator, *emu*.

Result: We find $\overline{QoC}(0.9) = -0.92$ indicating that incorporating the emulator block and running testbed components in different PCs increases the testbed overhead. From (5), this restricts V_{max} to $0.12m/s$.

B. QoC Assessment for Wifi Links

We assess the suitability of IEEE 802.11n (5GHz band) as the last-mile radio link for TCPS using the setup in Figure 21. Here, the IEEE 802.11n link is simulated in ns3. We determine the QoC value of the link by correcting for the testbed overhead. We plot the QoC values in Figure 22. For implementing an ideal TCPS, the last-mile radio link is expected to have $RTT < 200\mu s$ [32]. This transforms to a QoC requirement $> 0.69dB_{ideal}$. From Figure 22, we find the QoC of the radio link to be negative, indicating that its round trip latency is $> 1ms$. Thus we may conclude that IEEE802.11n has a limited performance to realize radio links for TCPS that require almost ideal performance, i.e., to support $V_{max} = 1m/s$.

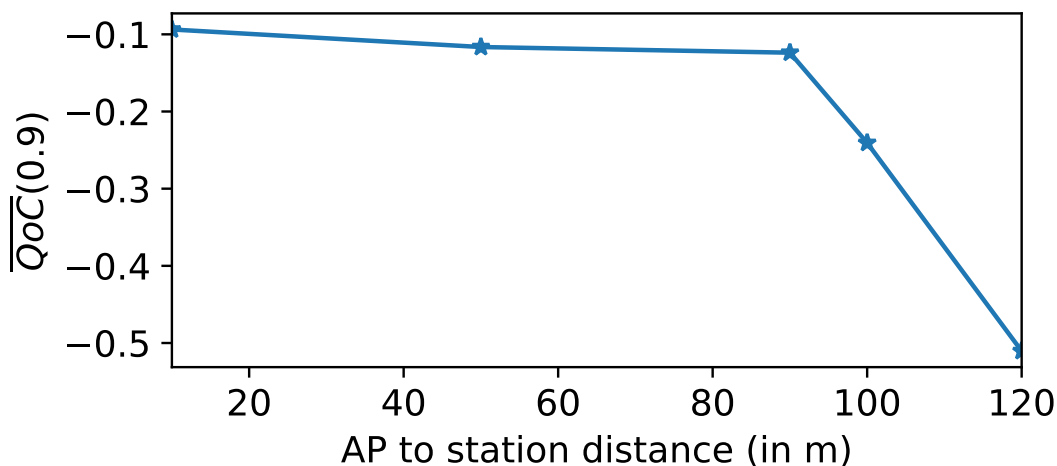


Fig. 22: QoC values for the IEEE802.11n link for different Access Point (AP) to station distances.

C. Evaluating the Impact of an Intercontinental Link

We understand that intercontinental links are not suited for TCPS that require $V_{max} = 1m/s$. However, we assess a real-world intercontinental link for TCPS to learn the V_{max} it can support. For the experiments, we replace PC#2 in Figure 21 with an intercontinental link. We place PC#1 and PC#3 at two university locations in Asia and Europe. We find $\overline{QoC}(.5) = -2.99$ and $V_{max} = 0.001m/s$. The resulting low V_{max} at low g_{spec} eliminates any practical use case for the implemented TCPS.

D. Comparing TCPS networks using QoC

We demonstrate how to use QoC to compare networks with different traffic conditions and different tactile endpoint locations. For evaluation, the network Figure 23 is simulated using Mininet [24]. The network represents the north-west subset of the USNET-24 topology. It consists of six switches managed by a central SDN controller. Tactile endpoints TE(Master) and TE(slave) connects to switches S1 and S6. Each switch in the network connects to a host, and every host communicates with every other host bidirectionally to simulate external traffic. The communication data is generated using the Linux tool iPerf. The SDN controller determines the routes between the hosts. Spanning tree protocol is used to avoid looping issues. For performing the QoC experiment, TE(Master) runs the PI controller, and TE(Slave) simulates step change. All host to switch links are made ideal, i.e., the links are configured to be of very low latency and very high bandwidth. Latencies and bandwidth of all links interconnecting the switches are set as variables for the user to set. The Mininet simulation is run on a server to reduce overheads.

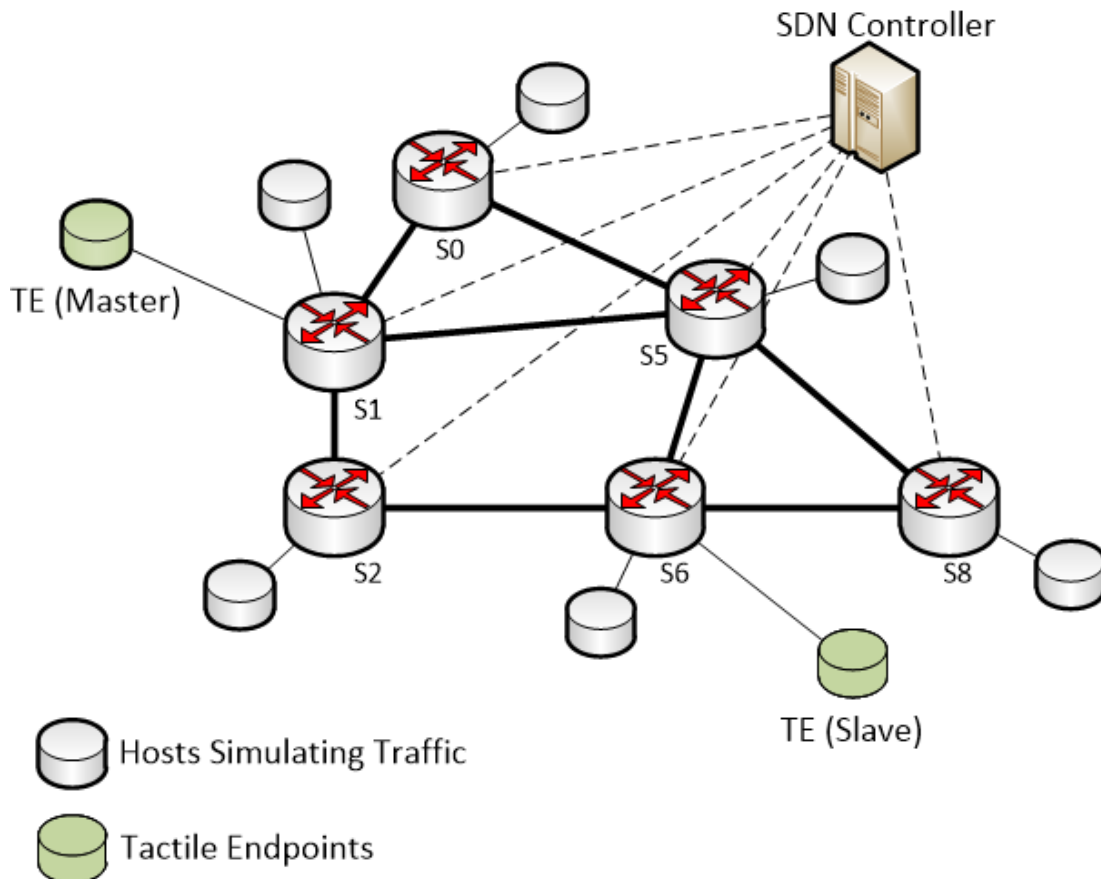


Fig. 23: Network topology simulated in Mininet.

1) *Effect of External Traffic*: In this experiment, for different traffic bandwidths simulated between host pairs, QoC is measured across the tactile endpoints. We fix delay and bandwidth for the links interconnecting the switches to $0.1ms$ and $10Mbps$ respectively. Figure 24 shows the QoC performance curve for different simulated traffic bandwidths. The host to host traffic bandwidth (H-H Traffic) in the legend corresponds to the unidirectional bandwidth simulated between host pairs. Figure 25 shows the corresponding calculated V_{max} for $g_{spec} = 0.9$.

Result: (i) We find QoC curves corresponding to H-H Traffic of 250Kbps and 500Kbps to be close. Because for both these cases, the effective bitrate of the simulated traffic is not enough to throttle the bandwidth of the links connecting tactile endpoints. (ii) QoC performance curve has a higher slope at higher values of g_{spec} . Thus, aiming for higher values of g_{spec} is costly w.r.t maintaining a higher value of QoC.

2) *Effect of Tactile Endpoint Locations*: In this experiment, we connect the tactile endpoints, TE(Master) and TE(Slave) to different switch pairs, and measure QoC across the tactile endpoints. We fix a delay of $0.1ms$ and bandwidth of $10Mbps$ for the links interconnecting the switches. We simulate H-H Traffic=625Kbps between the host pairs. Figure 26 shows the QoC performance curve for different tactile endpoint locations. TE(x,y) in the legend corresponds to the case where TE(Master) is connected to switch x and TE(Slave) to switch y . Figure 27 shows the corresponding calculated V_{max} for $g_{spec} = 0.9$.

Result: We find QoC performance curve corresponding to TE(0,8) has the lowest QoC values and hence, the lowest V_{max} . This is because the external traffic loads the route TE(Master)-S0-S5-S8-TE(Slave) more in comparison to other routes. The results are thus useful in predicting and how traffic in a network impact QoC performance depending on tactile endpoint locations.

E. QoC Measurement and Validation

In this experiment, we measure the combined QoC of a communication network and a connected robot in a non-haptic setting. We then use the QoC value to predict and quantify cybersickness.

1) *QoC Measurements*: For evaluation, the network in Figure 23 is simulated using Mininet [24]. TE(Master) runs the PI controller, and TE(Slave) simulates step change. The step change is simulated using the robot, IRB 4600, as described in Section III-C (see Figure 28). We use Virtual Robot Experimentation Platform (VREP) to simulate the robot [33]. We run VREP in TE(Slave) in the headless mode configuration, i.e., without GUI, to minimize the simulation overhead. A custom

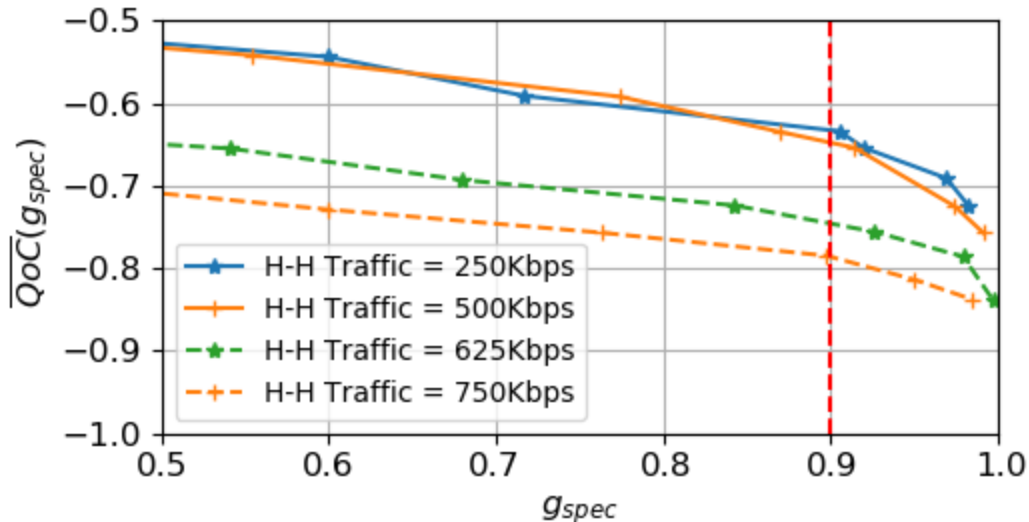


Fig. 24: QoC performance curves for different traffic conditions.

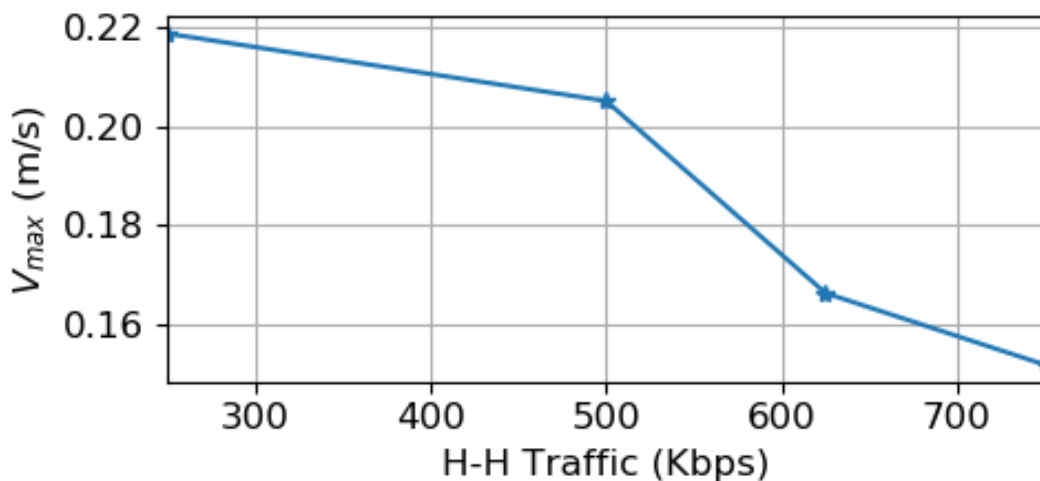


Fig. 25: V_{max} for $g_{spec} = 0.9$ for different traffic conditions.

written python script interfaces the network socket of TE(Slave) with VREP. We configured the delay and bandwidth of the links interconnecting the switches to $5ms$ and $10Mbps$ respectively. H-H Traffic is disabled.

Result: We measure QoC with and without the robot in place. Without the robot, we find $\overline{QoC}(1) = -1.42$, and with the robot, we find $\overline{QoC}(1) = -1.7$. From (5), this restricts V_{max} to $0.02m/s$.

2) *QoC Validation:* If QoC of the TCPS and dynamics of the operator's hand movements are known a priori, we can predict and quantify the operator side cybersickness using the QoC- V_{max} relation of (5) as follows. For example, if QoC of a network is $\overline{QoC}(1) = -0.1$ (i.e., $V_{max} = 0.1m/s$) and histogram of the operator's hand velocity suggest that the velocity is less than $0.1m/s$ for 90% of the time, we predict E to be 90%. Here E is used to quantify cybersickness. We define E as the percentage time during a TCPS operation, the error between the position of the operator's hand and the robot is within $|1mm|$.

For validating the above claim, we use the TCPS in Section VIII-E1, whose QoC and V_{max} is known ($\overline{QoC}(1) = -1.7$ and $V_{max} = 0.02m/s$). In the experimental setup, the operator side replays data corresponding to the hand movements of a surgeon performing the suturing operation [34]. At the teleoperator side, the robot (in VREP) replicates the surgeon's hand movement. Figure 29 shows the histogram of the operator's hand movement for a sampling frequency of $F_s = 30Hz$. We find that for 82% of the time, the velocity is less than V_{max} of $0.02m/s$. We thus expect E to be 82%. In Table V, we list the expected and the measured values of E for different F_s . We find the measured results to be very close to the expectation.

In the experiments, to measure E , at every $1/F_s$ seconds, the robot position is fed back to the operator side. At the operator

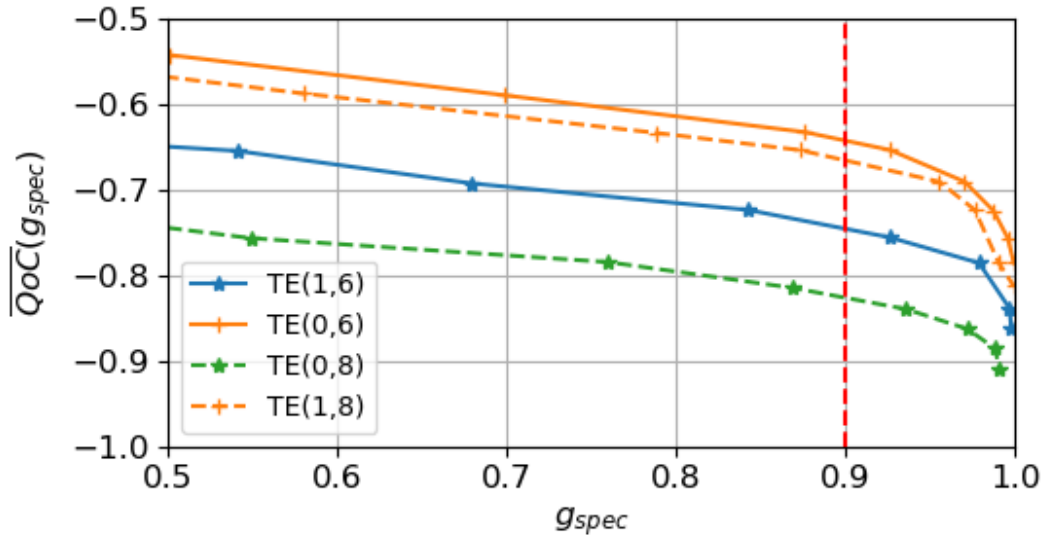


Fig. 26: QoC performance curves for different tactile end points.

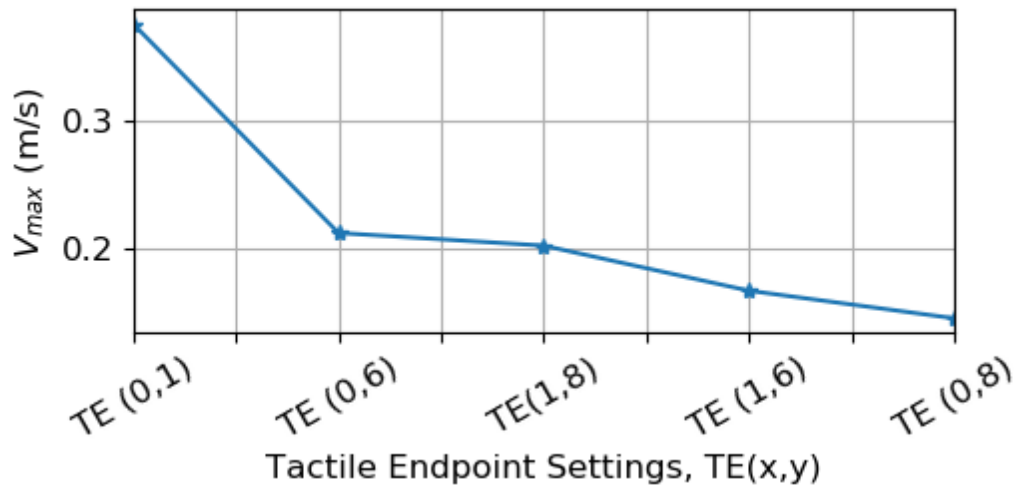


Fig. 27: V_{max} for $g_{spec} = 0.9$ for different traffic conditions.

side, at every instance of receiving the feedback, the error is calculated. For this, we subtract the robot position from the estimated position of the operator's hand at the receiving instance. From the error values, we find E by determining the percentage of time the error values stay within $|1mm|$. For this, we plot the normalized PDF of the error values and find the area under the curve between $-1mm$ and $1mm$.

TABLE V: Expected and measured values of E for different values of F_s .

| F_s (Hz) | Expected E (%) | Measured E (%) |
|------------|------------------|------------------|
| 40 | 77 | 81 |
| 30 | 82 | 86 |
| 20 | 88 | 92 |

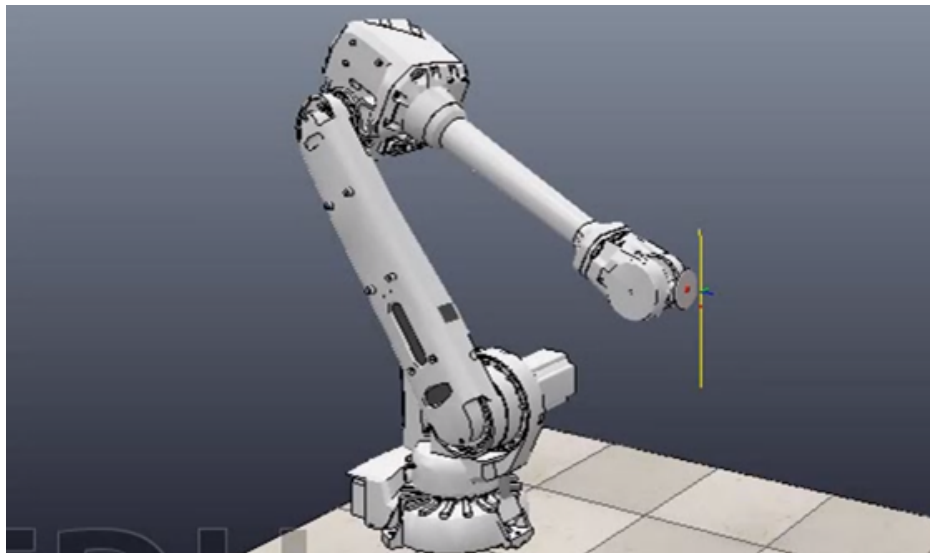


Fig. 28: Video frame captures the robot, IRB 4600, being actuated downwards along the vertical yellow line to simulate step change.

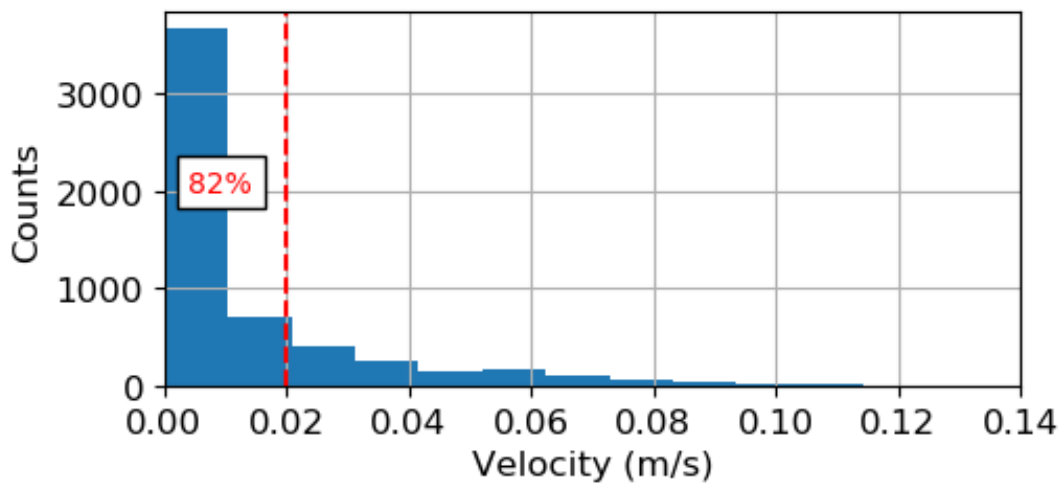


Fig. 29: Histogram of operator's hand velocity for $F_s = 30Hz$. For 82% of the time hand velocity is less than $V_{max} = 0.02m/s$.

IX. CONCLUSION

We have proposed a comprehensive evaluation methodology and metric for TCPS. Towards this, we have developed an evaluation model and have argued that we can determine the quality of a TCPS by evaluating its critical control loop. Depending on the application, we propose evaluating either the *kinematic-haptic* or the *kinematic-video* loop or both. Our evaluation methodology is an adaptation of the classical step response method. Here, we have replaced the human operator with a controller with known characteristics and have analyzed its response to slave side step changes. We have described methods to simulate step-change in scenarios where there exist haptic feedback and where there is not. These methods extend the use case of our proposed evaluation methodology to a broader spectrum of TCPS implementations. To quantify TCPS performance, we have developed a metric called *Quality of Control (QoC)*. Through simulations and experiments on a TCPS testbed, we have demonstrated the practicality of the proposed evaluation methodology and its usefulness in quantifying cybersickness.

REFERENCES

- [1] K. Polachan, P. T V, C. Singh, and D. Panchapakesan, "Quality of control assessment for tactile cyber-physical systems," in *2019 16th Annual IEEE International Conference on Sensing, Communication, and Networking (SECON)*, June 2019, pp. 1–9.
- [2] G. P. Fettweis, "The Tactile Internet: Applications and Challenges," *IEEE Vehicular Technology Magazine*, vol. 9, no. 1, pp. 64–70, March 2014.
- [3] ITU. (2014) The tactile internet. [Online]. Available: <https://www.itu.int/en/ITU-T/techwatch/Pages/tactile-internet.aspx>
- [4] A. N, A. S M, K. Polachan, P. T V, and C. Singh, "An end to end tactile cyber physical system design," in *2018 4th International Workshop on Emerging Ideas and Trends in the Engineering of Cyber-Physical Systems (EITEC)*, April 2018, pp. 9–16.

- [5] J. J. LaViola, Jr., "A Discussion of Cybersickness in Virtual Environments," *SIGCHI Bull.*, vol. 32, no. 1, pp. 47–56, Jan. 2000. [Online]. Available: <http://doi.acm.org/10.1145/333329.333344>
- [6] A. Aijaz, Z. Dawy, N. Pappas, M. Simsek, S. Oteafy, and O. Holland, "Toward a Tactile Internet Reference Architecture: Vision and Progress of the IEEE P1918.1 Standard," 2018.
- [7] K. Antonakoglou, X. Xu, E. Steinbach, T. Mahmoodi, and M. Dohler, "Towards Haptic Communications over the 5G Tactile Internet," *IEEE Communications Surveys Tutorials*, pp. 1–1, 2018.
- [8] D. V. D. Berg, R. Glans, D. D. Koning, F. A. Kuipers, J. Lugtenburg, K. Polachan, P. T. Venkata, C. Singh, B. Turkovic, and B. V. Wijk, "Challenges in Haptic Communications Over the Tactile Internet," *IEEE Access*, vol. 5, pp. 23 502–23 518, 2017.
- [9] A. Hamam and A. E. Saddik, "Evaluating the Quality of Experience of haptic-based applications through mathematical modeling," in *2012 IEEE International Workshop on Haptic Audio Visual Environments and Games (HAVE 2012) Proceedings*, Oct 2012, pp. 56–61.
- [10] Y. Kusunose, Y. Ishibashi, N. Fukushima, and S. Sugawara, "QoE assessment in networked air hockey game with haptic media," in *2010 9th Annual Workshop on Network and Systems Support for Games*, Nov 2010, pp. 1–2.
- [11] M. A. Jaafreh, A. Hamam, and A. E. Saddik, "A framework to analyze fatigue for haptic-based tactile internet applications," in *2017 IEEE International Symposium on Haptic, Audio and Visual Environments and Games (HAVE)*, Oct 2017, pp. 1–6.
- [12] A. Tatematsu, Y. Ishibashi, N. Fukushima, and S. Sugawara, "QoE assessment in haptic media, sound and video transmission: Influences of network latency," in *2010 IEEE International Workshop Technical Committee on Communications Quality and Reliability (CQR 2010)*, June 2010, pp. 1–6.
- [13] N. Sakr, N. D. Georganas, and J. Zhao, "A Perceptual Quality Metric for Haptic Signals," in *2007 IEEE International Workshop on Haptic, Audio and Visual Environments and Games*, Oct 2007, pp. 27–32.
- [14] C. G. Corrêa, D. M. Tokunaga, E. Ranzini, F. L. S. Nunes, and R. Tori, "Haptic Interaction Objective Evaluation in Needle Insertion Task Simulation," in *Proceedings of the 31st Annual ACM Symposium on Applied Computing*, ser. SAC '16. New York, NY, USA: ACM, 2016, pp. 149–154.
- [15] R. Chaudhari, E. Steinbach, and S. Hirche, "Towards an objective quality evaluation framework for haptic data reduction," in *2011 IEEE World Haptics Conference*, June 2011, pp. 539–544.
- [16] K. Polachan, T. V. Prabhakar, C. Singh, and F. A. Kuipers, "Towards an Open Testbed for Tactile Cyber Physical Systems," in *11th International Conference on Communication Systems & Networks, (COMSNETS)*, 2019.
- [17] D. J. Levitin, K. MacLean, M. Mathews, L. Chu, and E. Jensen, "The perception of cross-modal simultaneity (or the Greenwich Observatory Problem revisited)," *AIP Conference Proceedings*, vol. 517, no. 1, pp. 323–329, 2000.
- [18] J. M. Silva, M. Orozco, J. Cha, A. E. Saddik, and E. M. Petriu, "Human Perception of Haptic-to-video and Haptic-to-audio Skew in Multimedia Applications," *ACM Trans. Multimedia Comput. Commun. Appl.*, vol. 9, no. 2, pp. 9:1–9:16, May 2013.
- [19] A. Aijaz, M. Dohler, A. H. Aghvami, V. Friderikos, and M. Frodigh, "Realizing the Tactile Internet: Haptic Communications over Next Generation 5G Cellular Networks," Accepted for publication in *IEEE Wireless Communications*, dec 2015.
- [20] E. Steinbach, M. Strese, M. Eid, X. Liu, A. Bhardwaj, Q. Liu, M. Al-Jaafreh, T. Mahmoodi, R. Hassen, A. El Saddik, and O. Holland, "Haptic Codecs for the Tactile Internet," *Proceedings of the IEEE*, vol. 107, no. 2, pp. 447–470, Feb 2019.
- [21] E. Steinbach, S. Hirche, M. Ernst, F. Brandi, R. Chaudhari, J. Kammerl, and I. Vittorias, "Haptic communications," *Proceedings of the IEEE*, vol. 100, no. 4, pp. 937–956, 2012.
- [22] Eckehard Steinbach, "Haptic Communication for the Tactile Internet," Tech. Rep., 2017. [Online]. Available: <http://ew2017.european-wireless.org/wp-uploads/2017/05/keynotes-Steinbach-EW2017.pdf>
- [23] ns-3. (2018) ns-3. [Online]. Available: <https://www.nsnam.org>
- [24] Mininet. (2019) Mininet. [Online]. Available: <http://mininet.org/>
- [25] G. Buttazzo, M. Velasco, and P. Mart, "Quality-of-control management in overloaded real-time systems," *IEEE Transactions on Computers*, vol. 56, no. 2, pp. 253–266, 2007.
- [26] G. Buttazzo, M. Velasco, P. Marti, and G. Fohler, "Managing quality-of-control performance under overload conditions," *Proceedings. 16th Euromicro Conference on Real-Time Systems, 2004. ECRTS 2004.*, pp. 53–60, July 2004.
- [27] Y. C. Tian and L. Gui, "QoC elastic scheduling for real-time control systems," *Real-Time Systems*, vol. 47, no. 6, pp. 534–561, 2011.
- [28] E. Bini and A. Cervin, "Delay-aware period assignment in control systems," *Proceedings - Real-Time Systems Symposium*, pp. 291–300, 2008.
- [29] A. Aminifar, *Analysis, Design, and Optimization of Embedded Control Systems*, 2016, no. 1746.
- [30] A. Aminifar, P. Eles, Z. Peng, A. Cervin, and K. E. Arzen, "Control-Quality-Driven Design of Embedded Control Systems with Stability Guarantees," *IEEE Design and Test*, vol. 35, no. 4, pp. 38–46, 2018.
- [31] A. Cervin, J. Eker, B. Bernhardsson, and K. E. Årzén, "Feedback-feedforward scheduling of control tasks," *Real-Time Systems*, vol. 23, no. 1-2, pp. 25–53, 2002.
- [32] G. Fettweis and S. Alamouti, "5G: Personal mobile internet beyond what cellular did to telephony," *IEEE Communications Magazine*, vol. 52, no. 2, pp. 140 – 145, February 2014.
- [33] Coppeliarobotics. (2018) V-rep virtual robot experimental platform. [Online]. Available: <http://www.coppeliarobotics.com/>
- [34] Y. Gao, S. S. Vedula, C. E. Reiley, N. Ahmidi, B. Varadarajan, H. C. Lin, L. Tao, L. Zappella, B. Bejar, D. D. Yuh, C. C. G. Chen, R. Vidal, S. Khudanpur, and G. D. Hager, "Jhu isi gesture and skill assessment working set (jigsaws) a surgical activity dataset for human motion modeling," *Modeling and Monitoring of Computer Assisted Interventions (M2CAI) MICCAI Workshop*, pp. 1–10, 2014.